Synthesis and Characterization of Organic Ligands and the Corresponding Ru Dyes for Dye-sensitized Solar Cells

Baharak Bakhshaei

A Thesis submitted to the Faculty of Graduate Studies in Partial Fulfillment of the Requirements for the Degree of Master of Science

Graduate Program in Chemistry
York University
Toronto, Ontario

December 2014

Abstract

Ru(II) complexes have been of great interest as dyes for Dye-Sensitized Solar Cells (DSSCs), where they absorb solar energy and inject an electron into the conduction band of a semiconductor to start the process. The requirements for efficient light capture and electron injection include having a wide absorption envelope, the presence of a surface-anchoring group and appropriate HOMO and LUMO levels. In this thesis: A novel bidentate ligand is introduced and the synthesis of its various derivatives are explored as well as the synthesis of homoleptic and heteroleptic Ru complexes followed by their characterization using ^{1}H-NMR, ^{13}C-NMR, ESI-MS, EA, FT-IR and UV-visible spectroscopy.

Acknowledgments

I would like to deeply thank my supervisor Professor Pierre G. Potvin for accepting me to join his group and work on his interesting research, for always being there to help me overcome challenges and for trusting me and giving me the opportunity to gain precious experience supervising others.

I also would like to thank Professors Sylvie Morin and Jennifer Chen for the constructive comments and suggestions, Dr. Howard Hunter for helping with the NMR analysis, Professor Derek Wilson's group for helping with the Mass Spec analysis and the York University Chemistry Department staff that helped me throughout my research process.

Lastly I would like to thank my soulmate and the love of my life, my husband, David J. Baldesarra, who has supported me for the past seven years through the ups and downs of graduate and undergraduate work and given me courage and strength whenever I needed it.

Table of Contents

List of Abbreviations

COSY	Correlated Spectroscopy
d	Doublet
DCM	Dichloromethane
DEPT	Distortionless Enhancement by Polarization Transfer
DMF	N,N-Dimethylformamide
DMFDMA	N,N-Dimethylformamide dimethyl acetal
DMSO	Dimethylsuphoxide
EDTA	Ethylenediaminetetraacetic acid
Et	Ethyl
fac	Facial
g	Gram
h	Hour
HOMO	Highest Occupied Molecular Orbital
HSQC	Heteronuclear Single Quantum Coherence
LUMO	Lowest Unoccupied Molecular Orbital
m	Multiplet
Me	Methyl
mer	Meridional
mg	Milligram
mL	Millilitre
mmol	Millimole

MS	Mass Spectrometry
NMR	Nuclear Magnetic Resonance
OAc	Acetate
^{i}pr	Isopropyl
q	Quartet
s	Singlet
SOMO	Singly Occupied Molecular Orbital
t	Triplet
TEA	Triethylamine
TFA	Trifluoroacetic acid
THF	Tetrahydrofuran
UV-vis	Ultraviolet-visible

List of Figures

Chapter One: Introduction

1.1. Renewable Energy: Importance and Limitations

The issue of global warming and the need for renewable energy has been the centre of attention globally for the past several decades. The correlation between population growth and the incremental cost increase of natural resources has led the focus towards the development of renewable energy.[1] According to the 2014 Annual Energy Outlook, solar and wind energy are expected to remain the main sources of renewable energy for at least the next two decades. It further stated that, while the cost of photovoltaics has declined over the past decade, the changes in the cost of future development remains uncertain.[2] Other than the rising cost of the carbon-based fuels, there is an issue with the limited amount of these resources that needs much attention. Evidently, continuing with the same usage of the resources over time will cause them to inevitably run out, hence the development of a replacement technology to provide clean and competitive energy is a necessity.[1,3]

---

1 Hoffert, M. I., Caldeira, K., Jain, A. K., Haites, E. F., Harvey, L. D. D., Potter, S. D., Wuebbles, D. J. (1998). Energy implications of future stabilization of atmospheric CO2 content. *Nature (London), 395*(6705), 881-884. doi:10.1038/27638

2 Bredehoeft, G. (2014). (No. #DOE/EIA-0383(2014)). USA: US Energy Information Administration.

3 Rogelj, J., McCollum, D. L., Reisinger, A., Meinshausen, M., & Riahi, K. (2013). Probabilistic cost estimates for climate change mitigation. *Nature, 493*(7430), 79-83.

1.2. Photovoltaics and the Discovery of Dye-sensitized Solar Cells

As stated earlier, solar energy has become one of the most attractive topics of research in recent years due to the depletion of carbon-based fuels.[2] The photovoltaic effect was first discovered by the French physicist Alexandre-Edmond Becquerel in 1839.[4] This process being the basis of all modern day solar cells involves the production of electricity in a certain material by exposing it to sunlight. Furthermore, the current commercially available technologies consisting of the silicon-based photovoltaics are very costly, which has led the search towards a relatively new family of solar cells known as the dye-sensitized solar cells or DSSCs.[5]

In 1968, Heinz Gerischer, the thesis advisor of nobel laureate Gerhard Ertl, proposed the idea of charge injection from an organically synthesized dye into the conduction band of a semi-conductor.[6] Twenty three years after this discovery, Michael Grätzel from the École Polytechnique Fédérale de Lausanne together with Brian O'Regan co-invented the first ever dye-sensitized solar cell.[7]

---

4. Williams (1960). "Becquerel Photovoltaic Effect in Binary Compounds". *The Journal of Chemical Physics* **32** (5): 1505–1514. Bibcode:1960JChPh..32.1505W. doi:10.1063/1.1730950

5 Ponnampalam, Dino. DSSC – Transforming A Solar Cell. Energy Trend: Solar.2011-12-02. <http://www.energytrend.com/DSSC_20111202>. Access Date: 2012-03-30.

6 Gerischer, H.; Michel-Beyerle, M.; Rebentrost, F.; Tributsch, H. Sensitization of charge injection into semiconductors with large band gap. *Electrochim. Acta* 1968, *13*, 1509-15.

7 O'Regan, B.; Graetzel, M. A low-cost, high-efficiency solar cell based on dye-sensitized colloidal titanium dioxide films. Nature (London) 1991, 353, 737-40.

In a Grätzel DSSC, light is absorbed by a sensitizer which is anchored to semi-conductor TiO_2 nanocrystallites through groups such as carboxylates, phosphonates and hydroxamates.[8] This is in contrast to conventional systems where the semiconductor acts as the light absorber as well as the charge carrier. Photo-induced electron injection occurs at the interface where the charge is transferred from the dye into the conduction band of the semiconductor. The dye is then regenerated to form a closed circuit.[7]

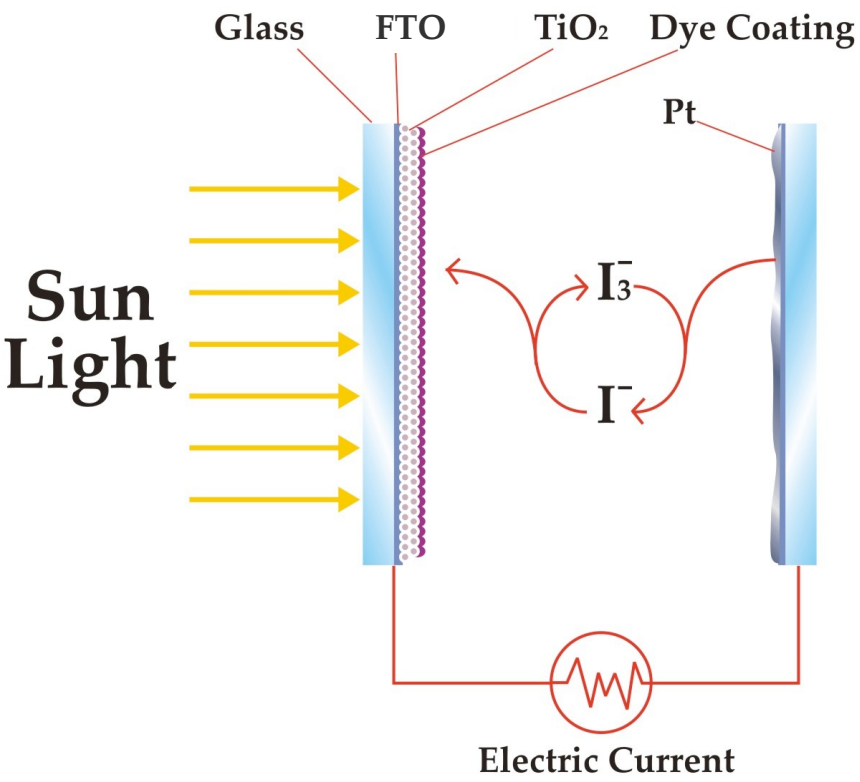

Figure 1.2.1. *A simple depiction of the structure of a dye-sensitized solar cell based on the original Grätzel design.*

8 Sekar, N.; Gehlot, V. Y. Metal complex dyes for dye-sensitized solar cells: recent developments. Resonance 2010, 15, 819-831.

Light is absorbed by the dye complex over a wide range of wavelengths from UV to near IR regions for the maximum efficiency. Ideally the dye sensitizer is designed to absorb all the light below the threshold wavelength of 920 nm while having a sufficiently high redox potential for constant regeneration.[2]

Figure 1.2.1 presents a simplified diagram of a DSSC originally introduced by Grätzel. The design involves two transparent glass plates which sandwich the other contents of the cell. A transparent conducting oxide (TCO) layer is used as a substrate for the TiO_2 photoelectrode. For the purpose of best performance, the TCO must be fully transparent with low sheet resistance. The sheet resistance should also be temperature independent since the process of attaching the TiO_2 on to the electrode takes place at a high temperature. The most popular TCO for the purpose of DSSCs is FTO (fluorine-doped SnO_2). Indium-tin oxide is also used however due to its increased sheet resistance at high temperatures, it is not the best material in DSSC applications.[9]

Titanium oxide thin film is affixed on the TCO layer by means of either the doctor blade technique or by screen printing.[10] The best thickness for the TiO_2 nano-crystallite is determined to be 13-14 μm and porosity of 60-70%.[10]

---

9 Hara, Kohjiro, and Hironori Arakawa. "Dye-Sensitized Solar Cells".John Wiley & Sons Ltd , 2003. 663-700. Print.

10 Barbe, C. J.; Arendse, F.; Comte, P.; Jirousek, M.; Lenzmann, F.; Shklover, V.; Gratzel, M. Nanocrystalline titanium oxide electrodes for photovoltaic applications. *J Am Ceram Soc* 1997, *80*, 3157-3171.

In order to apply the dye-sensitizer to the TiO_2 surface, the coated plate is exposed to a known concentration of a dye solution for 24 hours during which the dye complex becomes covalently bound to the TiO_2 surface. The other plate is coated with a layer of platinum to act as the counter electrode. An electrolyte solution (e.g. I^-/I_3^-) is placed in between the two plates and the assembly is sealed to prevent leakage.[10,11]

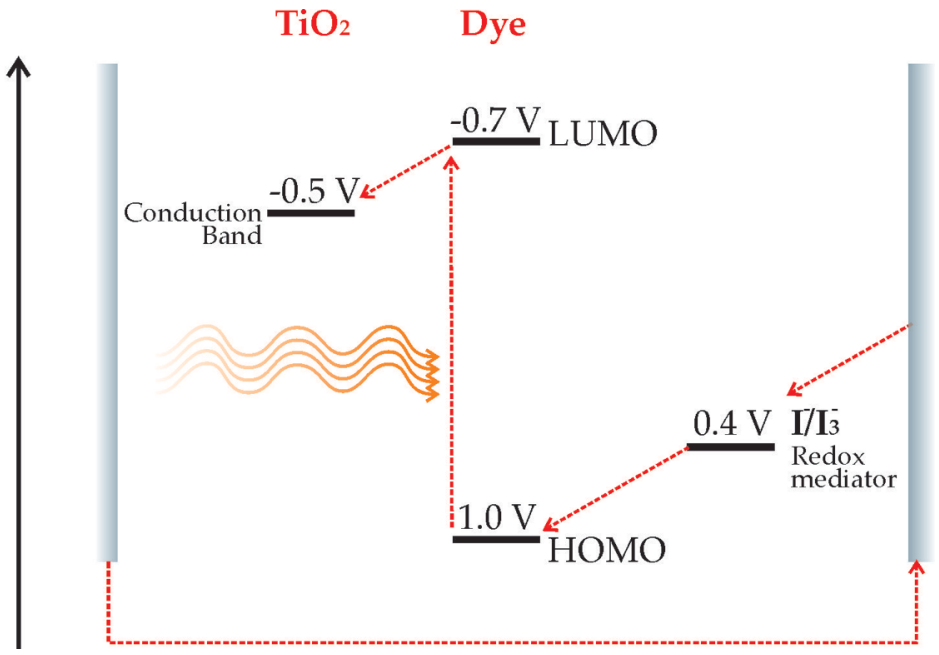

Figure 1.2.2. *The acceptable energy levels of an arbitrary dye at oxidized and reduced states.*

11 Holliman, P. J.; Mohsen, M.; Connell, A.; Davies, M. L. et al. Ultra-fast co-sensitization and tri-sensitization of dye-sensitized solar cells with N719, SQ1 and triarylamine dyes. *J. Mater. Chem.* 2012, *22*, 13318-13327.

Figure 1.2.2 shows an energy diagram of the process involved with the excitation of the dye, electron injection into the conduction band of TiO_2 and the regeneration of the dye by the I^-/I^-_3 redox mediator. The voltages are estimated based on the Lever parameters for a homoleptic Ru complex with three bidentate ligands consisting of a pyrazole and a pyridine group using NHE as the reference.

There has been extensive research put in studying various other types of dyes for DSSCs over the years[12], and these include dyes generated from the use of other metals such as Fe[13], Os[14] and Ir[15]. More recently the generation of organic dyes have shown promising results with highly efficient dyes that operate using a Co(II/III) tris(bipyridyl) redox mediator.[16] One of the most successful recent designs involves the use of porphyrin-type zinc complexes that also operate with the Co(II/III) tris(bipyridyl) electrolyte which also have shown improved efficiencies that are comparable to Ru-based dyes.[17]

---

12 Polo, A. S.; Itokazu, M. K.; Murakami Iha, N. Y. Metal complex sensitizers in dye-sensitized solar cells. *Coord. Chem. Rev.* 2004, *248*, 1343-1361.

13 Ferrere, S. New photosensitizers based upon Fe(L)2(CN)2] and Fe(L)3] (L = substituted 2,2'-bipyridine): yields for the photosensitization of TiO2 and effects on the band selectivity. *Chem. Mater.* 2000, *12*, 1083-1089.

14 Altobello, S.; Argazzi, R.; Caramori, S.; Contado, C.; Da Fre, S.; Rubino, P.; Chone, C.; Larramona, G.; Bignozzi, C. A. Sensitization of Nanocrystalline TiO2 with Black Absorbers Based on Os and Ru Polypyridine Complexes. *J. Am. Chem. Soc.* 2005, *127*, 15342-15343.

15 Ning, Z.; Zhang, Q.; Wu, W.; Tian, H. Novel iridium complex with carboxyl pyridyl ligand for dye-sensitized solar cells: High fluorescence intensity, high electron injection efficiency? *J. Organomet. Chem.* 2009, *694*, 2705-2711.

16 Feldt, S. M.; Gibson, E. A.; Gabrielsson, E.; Sun, L.; Boschloo, G.; Hagfeldt, A. Design of Organic Dyes and Cobalt Polypyridine Redox Mediators for High-Efficiency Dye-Sensitized Solar Cells. *J. Am. Chem. Soc.* 2010, *132*, 16714-16724.

17 Yella, A.; Lee, H.; Tsao, H. N.; Yi, C.; Chandiran, A. K.; Nazeeruddin, M. K.; Diau, E. W.; Yeh, C.; Zakeeruddin, S. M.; Graetzel, M. Porphyrin-Sensitized Solar Cells with Cobalt (II/III)-Based Redox Electrolyte Exceed 12% Efficiency. *Science (Washington, DC, U. S.)* 2011, *334*, 629-634.

1.3. Design of the Dye Complex

The first Ru complex used as a dye sensitizer by O'Regan and Grätzel contained two bidentate ligands and two CN groups. The bidentate ligands were 2,2'-bipyridine-4,4'-dicarboxylic acid (dcbpy) and 2,2'-bipyridine (bpy).[18] These chelating compounds are known to promote metal-to-ligand charge-transfer (MLCT) when coordinated to a metal centre. MLCT involves transitions from metal-centred orbital to ligand-centred π^* orbital, where the HOMO is delocalized over the electron-rich region (the metal) and the LUMO is delocalized over the electron-poor region which in this case is the ligand bearing the anchoring groups.[19,20]

This dye belongs to a class of compounds that are chromophores absorbing light at ultraviolet to near-infrared wavelengths which can donate an electron to the semi-conductor whose conduction band lies slightly below the SOMO energy level of the dye complex at the excited state.[21] The goal in synthesis of these dyes is to achieve a panchromatic dye, meaning a dye that would absorb light at every wavelength. This is achieved by having a variety of

---

18 B. O'Regan, M. Grätzel, Nature 335 (1991) 737; (b) M. Grätzel, Nature 414 (2001) 338–344.

19 Anderson, P. A.; Strouse, G. F.; Treadway, J. A.; Keene, F. R.; Meyer, T. J. Black MLCT Absorbers. *Inorg. Chem.* 1994, *33*, 3863-4.

20 Nazeeruddin, M. K.; Pechy, P.; Renouard, T.; Zakeeruddin, S. M.; Humphry-Baker, R.; Comte, P.; Liska, P.; Cevey, L.; Costa, E.; Shklover, V.; Spiccia, L.; Deacon, G. B.; Bignozzi, C. A.; Gratzel, M. Engineering of efficient panchromatic sensitizers for nanocrystalline TiO(2)-based solar cells. *J. Am. Chem. Soc.* 2001, *123*, 1613-24.

21 Wang, S.; Wu, K.; Ghadiri, E.; et al. Engineering of thiocyanate-free Ru(II) sensitizers for high efficiency dye-sensitized solar cells. Chem. Sci., 2013,4, 2423-2433.

absorption transitions from the HOMO and sub-HOMO to the LUMO and supra-LUMO levels and then to the CB. The two key factors are a low-lying π^* and destabilization of the metal e_g through strong σ donating ligands to prevent the non-radiative decay of the excited state straight to the ground state.[15] Some analogues of the original Ru dye are shown in *Figure 1.3.1*. These displayed further improvement in the efficiency of the DSSCs.[22]

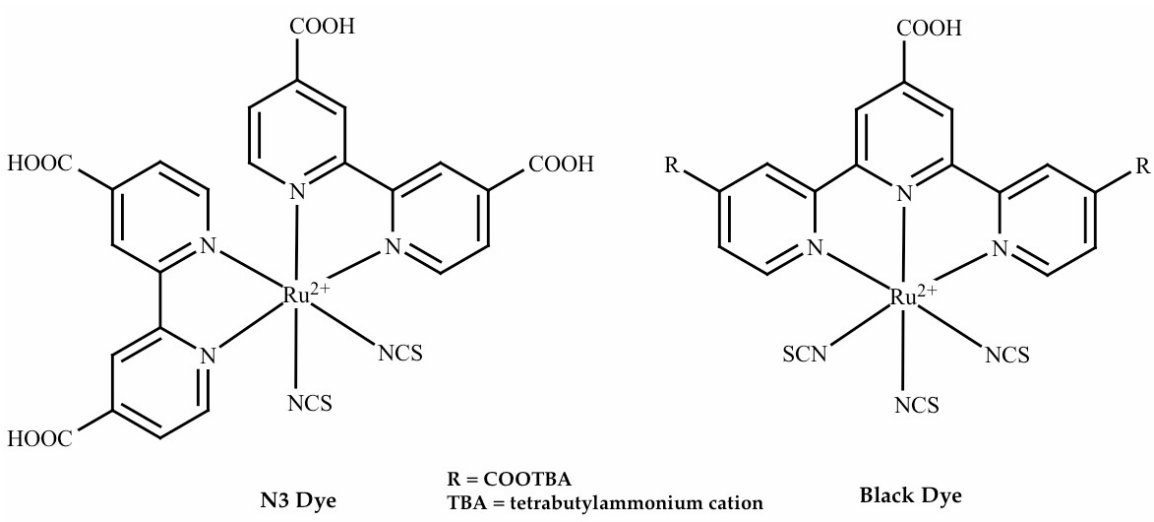

Figure 1.3.1. *The two most efficient dyes originally introduced by Grätzel. Black dye (right) is one of the most efficient dyes to date at 10% efficiency.*

A group of most efficient dyes that have been introduced up to now have been of the **N3** dye generation. These champion dyes have shown efficiencies

22 Ozawa, H.; Shimizu, R.; Arakawa, H. Significant improvement in the conversion efficiency of black-dye-based dye-sensitized solar cells by cosensitization with organic dye. RSC Adv. 2012, 2, 3198-3200.

slightly above 10%. The ligands with more conjugated systems enhance the π to π^* electron transitions and this was observed with the **Black Dye** being one of the most efficient dyes ever prepared. More recent studies have shown that the thiocyanate groups that enhance the electron density at the metal centre are not the best in terms of long-term stability and efforts have been made to find alternatives to these mono-dentate labile groups. These include the development of cyclometalated complexes that involve the use multi-dentate ligands in place of the labile mono-dentate ligands.[23]

In this thesis, a novel bidentate ligand is introduced and its various combinations with other bidentate and tridentate ligands are investigated for synthesis of homoleptic and heteroleptic complexes.

23 Kiyoshi, D.; Robson, P. and Berlinguette, C.; Cycloruthenated sensitizers: improving the dye-sensitized solar cell with classical inorganic chemistry principles. Dalton Trans., 2012, 41, 7814.

1.4. Intermediates, Ligands and Target Complexes

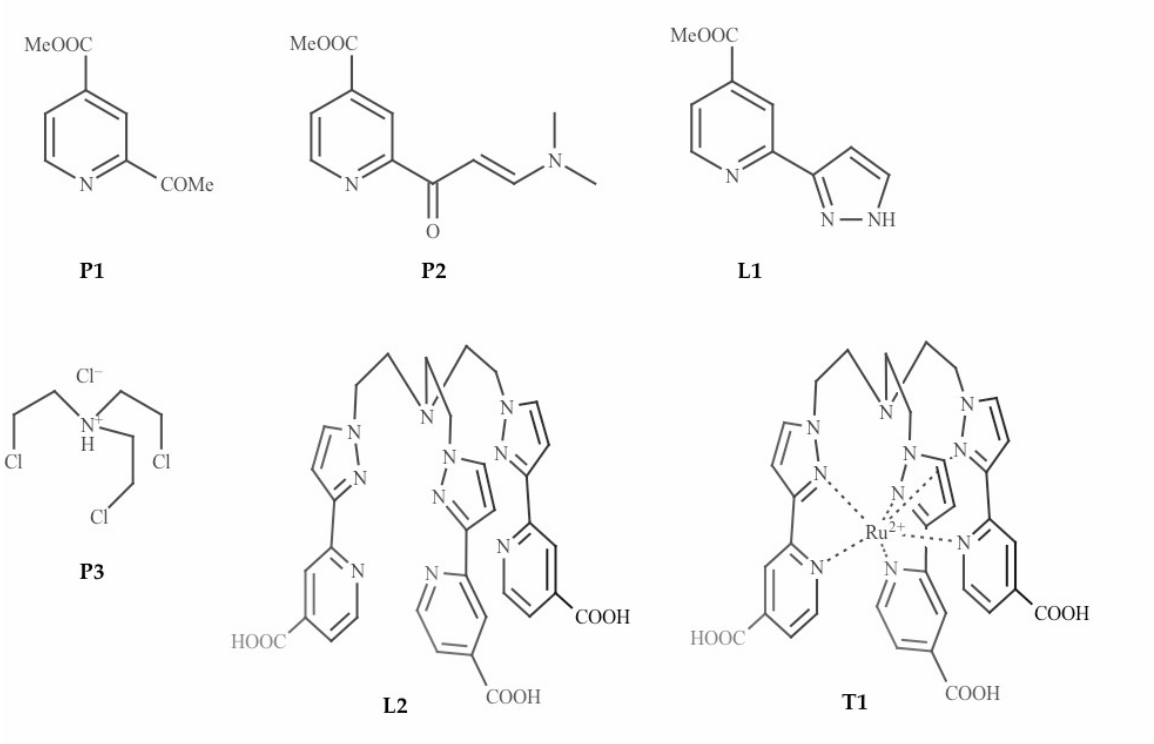

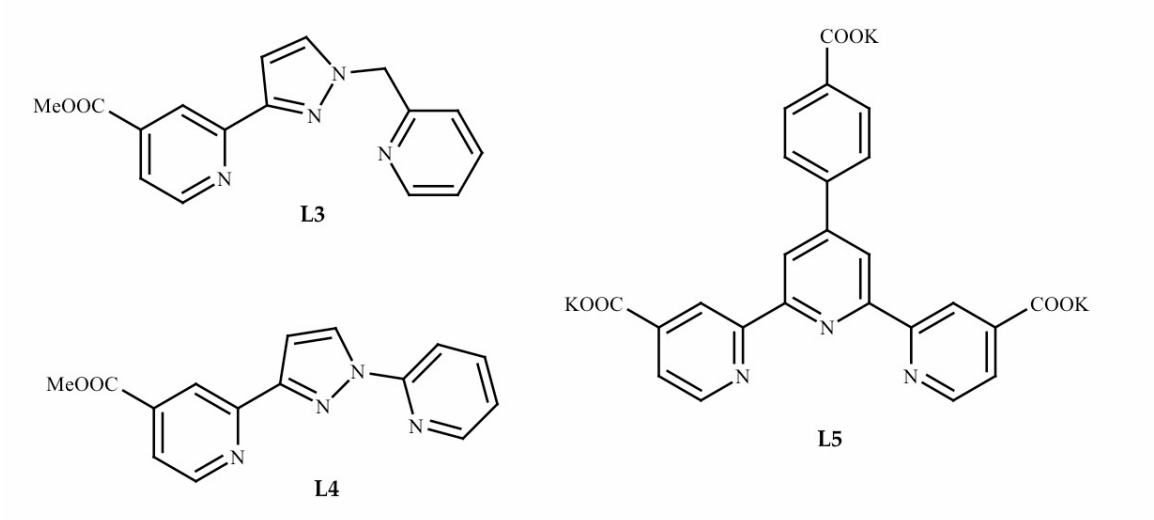

1.4. Intermediates, Ligands and Target Complexes continued

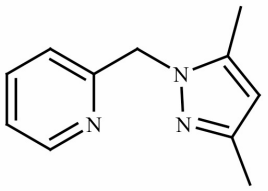

L7

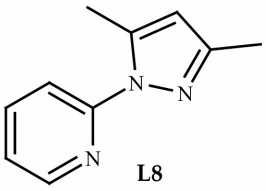

L8

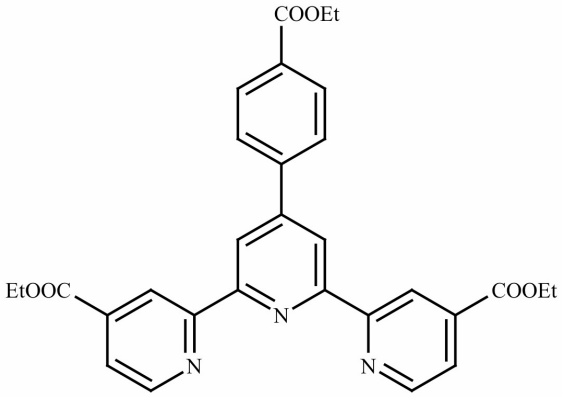

L6

Chapter Two: Experimental

2.1. General Procedures

All the reagents were purchased from Aldrich unless specified otherwise. All solvents used were from Caledon Labs Inc. NMR analysis was performed using Bruker ARX 300, 400 and 600 MHz spectrometers. UV-Visible analysis was performed using a Cary 100 Bio spectrophotometer. FT-IR spectra were obtained using a Nicolet 380 spectrophotometer. Mass analysis was performed by Wilson's lab York University using Sciex QStar Elite Quadrupole time-of-flight (Qq-TOF) mass spectrometer. Elemental Analysis was carried out by Guelph Chemical Laboratories. All air-sensitive reactions were performed under argon using a standard Schlenk techniques.

2.2. Synthesis of Methyl 2-Acetylisonicotinate (**P1**)

To 150 mL of acetonitrile, 14.0 mL (0.116 mol) of methyl isonicotinate were added followed by the addition of 68.5 mL (0.500 mol) of paraldehyde, 28.6 mL, 40% solution (0.222 mol) of ^{t}BuOOH, 7.8 mL of TFA (0.100 mol) and 1 g (3.56 mmol) of $FeSO_4 \bullet 6H_2O$. The mixture was heated at reflux for precisely two hours. The acetonitrile was then distilled off and the remaining liquid

was mixed with approximately 40 mL of toluene and this was washed four times with water. The toluene was then removed and the remaining liquid was placed under high vacuum for a few hours whereupon the product would solidify. Yield 60%. The colour of the product varied from a light cream colour to dark brown. ^{1}H-NMR (300 MHz, $CDCl_3$, 25 °C) δ/ppm: 8.86 (d, 1H, J = 4.9), 8.58 (s, 1H), 8.05 (d, 1H, J = 4.9), 4.01 (s, 3H), 2.78 (s, 3H). The chemical shifts observed correspond to the values recorded in the literature.[24]

2.3. Synthesis of Dimethylamino Precursor (**P2**)

To 2.496 g (13.9 mmol) of dry **P1** dissolved in 15 mL of toluene, 2.86 mL (20.9 mmol) of DMFDMA were added. The mixture was heated at reflux over night (~20 h).[25] The solvent was then removed and the remaining material was dried under high vacuum to obtain a golden brown solid in quantitative yield. ^{1}H-NMR (300 MHz, $CDCl_3$, 25 °C) δ/ppm: 8.78 (d, 1H, J = 4.9), 8.67 (s, 1H), 8.03 (d, 1H, J = 12.5), 7.94 (d, 1H, J = 4.9), 6.48 (d, 1H, J = 12.5), 3.97 (s, 3H), 3.22 (s, 3H), 3.03 (s, 3H).

---

24 Ishihara, M.; Tsuneya, T.; Shiga, M.; Kawashima, S.; Yamagishi, K.; Yoshida, F.; Sato, H.; Uneyama, K. New pyridine derivatives and basic components in spearmint oil (Mentha gentilis f. cardiaca) and peppermint oil (Mentha piperita). *J. Agric. Food Chem.* 1992, *40*, 1647-55.

25 Develay, S.; Blackburn, O.; Thompson, A. L.; Williams, J. A. G. Cyclometalated platinum(II) complexes of pyrazole-based, N=C=N-coordinating, terdentate ligands: the contrasting influence of pyrazolyl and pyridyl rings on luminescence. Inorg. Chem. 2008, 47, 11129-42.

2.4. Synthesis of Pyrazolepyridine (**L1**) Using Hydrazine Hydrate

Precursor **P2** (2.114 g, 9.03 mmol) was dissolved in 50 mL of reagent grade methanol followed by the addition of 0.48 mL (9.93 mmol) a hydrazine hydrate. The mixture was heated at reflux for three hours. The methanol was then distilled off and a dark brown oily material was obtained. The product was extracted from the oily material by a solid/liquid extraction using chloroform. All the chloroform extracts were combined and dried to obtain a light brown solid in 57% yield. ^{1}H-NMR (300 MHz, $CDCl_3$, 25 °C) δ/ppm: 8.77 (d, 1H, J = 5.0), 8.33 (s, 1H), 7.76 (d, 1H, J = 5.0), 7.70 (d, 1H, J = 2.1), 6.91 (d, 1H, J = 2.1), 3.97 (s, 3H). ^{13}C-NMR (400 MHz, $CDCl_3$, 25 °C) δ/ppm: 165.4, 151.0, 150.1, 145.8, 138.2, 135.7, 121.6, 119.4, 103.9, 52.7.

2.5. Synthesis of Pyrazolepyridine (**L1**) Using Anhydrous Hydrazine

Precursor **P2** (0.2343 g, 1 mmol) was dissolved in 10 mL of anhydrous methanol followed by the addition of 2 mL (2 mmol) of a 1 M THF solution of anhydrous hydrazine. The mixture was heated at reflux for five hours. The same workup as in section 2.4 were performed to result in a yield of 72%.

2.6. Synthesis of Tri(2-chloroethyl)ammonium Chloride (**P3**)

To a solution of 1.3 mL (10.0 mmol) triethanolamine in 20 mL of chloroform, 2.9 mL (40.0 mmol) of thionyl chloride was added and heated at reflux for four hours. The chloroform was distilled off and the remaining white solid was washed twice with acetone. The yield of the pure solid was 67%.[26]

2.7. Synthesis of Terpyridine Tricarboxylate Potassium Salt (**L5**)

In a solution prepared by mixing 7.2 mL of 15% KOH and 0.8 mL of concentrated NH_4OH in 8 mL of methanol, 0.430 g (2.40 mmol) of **P1** and 0.201 g (1.20 mmol) of methyl 4-formylbenzoate were added. The uniform solution was left at room temperature for 24 hours to yield a light cream

26 Wilson, E.; Tishler, M. Nitrogen mustards. *J. Am. Chem. Soc.* 1951, *73*, 3635-41.

precipitate in 30% yield. ^{1}H-NMR (400 MHz, TFA-d, 25 °C) δ/ppm: 10.29 (s, 2H), 10.15 (d, 2H), 9.80 (s, 2H), 9.50 (d, 2H), 9.08 (d, 2H), 8.85 (d, 2H).[27]

2.8. Synthesis of **L5** in Non-Aqueous Conditions (The Hanan Method)

In 10 mL of anhydrous methanol, 1.5 g of KOH (26.7 mmol) and 0.5 g of NH_4OAc (6.50 mmol) were mixed together and stirred until completely dissolved. Once a uniform solution was obtained, 0.179 g of **P1** (1.0 mmol) and 0.082 g of methyl 4-formylbenzoate (0.50 mmol) were added to the solution and stirred to dissolve. The mixture was left at room temperature for 24 hours to give a quantitative yield of a powdery tan coloured precipitate. The material was identical to the product obtained in the section 2.7.[28]

2.9. Synthesis of Terpyridine Triester (**L6**)

Dry **L5** (0.361 g, 0.651 mmol) was placed in 50 mL of anhydrous ethanol. Approximately 0.1 mL of (1 mmol) H_2SO_4 was added and the solution was

---

27 Vougioukalakis, G. C.; Stergiopoulos, T.; Kantonis, G.; Kontos, A. G.; Papadopoulos, K.; Stublla, A.; Potvin, P. G.; Falaras, P. Terpyridine- and 2,6-dipyrazinylpyridine-coordinated ruthenium(II) complexes: Synthesis, characterization and application in TiO2-based dye-sensitized solar cells. *J. Photochem. Photobiol. , A* 2010, *214*, 22-32.

28 Cooke, M. W.; Wang, J.; Theobald, I.; Hanan, G. S. Convenient one-pot procedures for the synthesis of 2,2':6',2''-terpyridine. *Synth. Commun.* 2006, *36*, 1721-1726.

heated overnight. The volume of the reaction mixture was reduced to ⅓ followed by the addition of a saturated solution of $NaHCO_3$ (20 mL) until neutrality as verified with pH paper then the rest of the methanol was evaporated off. About 40 mL of DCM were added to the aqueous solution and the contents were transferred to a separatory funnel with gentle swirling to separate the product (shaking causes an emulsion and loss of the product). The organic layers were combined and dried to give a 35% yield. ^{1}H-NMR (300 MHz, $CDCl_3$, 25 °C) δ/ppm: 9.31 (s, 2H), 9.07 (m, 2H), 8.94 (m, 2H), 8.20 (dd, 2H), 7.69 (m, 2H), 7.58 (s, 1H), 4.80 (d, 2H), 1.78 (t, 3H). The NMR chemical shifts match the reported values in the literature.[29]

2.10. Synthesis of Homoleptic Ru Complex with **L1**

In 30 mL of anhydrous ethanol, 0.305 g of **L1** (1.50 mmol) and 0.113 g of $RuCl_3 \bullet 3H_2O$ (0.50 mmol) were mixed and heated at reflux for three days. The reaction mixture was then cooled and dried and the solvent was replaced with methanol to which was added ~1.5 mL of acetyl chloride and the mixture was set to reflux for 24 hours. This is to reverse the trans-esterification that occurs in the previous step. The reaction mixture

29 Duprez, V.; Krebs, F. C. New carboxy-functionalized terpyridines as precursors for zwitterionic ruthenium complexes for polymer-based solar cells. *Tetrahedron Lett*. 2006, *47*, 3785-3789.

was concentrated and added drop wise to a concentrated aqueous solution of NH_4PF_6 to obtain a precipitate in 79% yield. ^{1}H-NMR (400 MHz, CD_3CN, 25 °C) δ/ppm: 12.06 (m, 1H), 8.61 (d, 1H), 7.75 (m, 3H), 7.37 (d, 1H), 3.94 (m, 3H). ^{13}C-NMR (400 MHz, CD_3CN, 25 °C) δ/ppm: 165.4, 165.2, 156.2, 156.1, 155.9, 155.8, 155.4, 155, 154.8, 154.4, 153.0, 152.8, 152.7, 152.4, 139.7, 135.7, 135.6, 135.5, 135.4, 125.3, 125, 124.6, 122.9, 122.6, 122.5, 122.3, 107.2, 107.1, 107, 106.9.

Chapter Three: Results and Discussion

3.1. Design of **L1**

L1 was designed to contain electron-rich and electron-poor regions within the same ligand. The electron-rich region being the pyrazole, a five-membered ring with 6π electrons, and the electron-poor region being the pyridine, a six-membered ring with the same number of π electrons. It is very important for the anchoring group to be near the pyridine group to enhance charge transfer to the conduction band of TiO_2 and provide a further electron-withdrawing effect on this electron-poor region. Another important factor involves having a π conjugation with the conduction band of TiO_2 and this is fulfilled through the π conjugation provided by the pyridine through the anchoring group.

In imitation of the push-pull effect in the Grätzel complex, one ligand typically acts as the electron density provider towards the electron deficient metal once it has undergone excitation. This tends to stabilize the excitation state and promote longer excitation lifetime for the excited electron and consequently higher efficiency in terms of electron injection into the conduction band of the TiO_2.

A Ru^{2+} complex with L1 is hypothesized to stabilize the excitation state of the complex by providing the electron density through the pyrazole substituent into the electron deficient Ru^{3+} hence lowering the energy of the excitation state. In the **Black Dye** model developed by the Grätzel group, this role is fulfilled by the three SCN groups attached to Ru and while this has proven to be one of the most efficient dyes to date, the SCN groups tend to undergo photo-substitution in which the SCNs are lost as SCN anions and this completely changes the absorption profile of the complex as well as its electron injection ability.[30]

Ligand **L1** can bind to TiO_2 through the carboxylate group either as a carboxylate or as an ester by trans-esterification. The carboxylate group is specifically designed on the position four of the pyridine of **L1**, which ultimately would allow the dye containing multiple **L1**s, to bind at more than one point to the TiO_2 layer thereby allowing for a high binding stability. This is in contrast to the carboxylate being placed at positions three or six that will result in steric congestion. For example in position three, it would engage in a strong steric interaction with the pyrazole ring and prevent the pyrazole and pyridine rings to be co-planar which would adversely affect the binding and the electronics of the complex. In the case of carboxylate placed at position six, there would be steric

30 Kiyoshi, D.; Robson, P. and Berlinguette, C.; Cycloruthenated sensitizers: improving the dye-sensitized solar cell with classical inorganic chemistry principles. Dalton Trans., 2012, 41, 7814.

interactions between units of **L1** around the same Ru, which would again cause poor binding ability and possibly improper electronics of the resulting complex. The last position left available would be position five which is probably fine in terms of the geometry of the complex not causing any steric congestions.

The goal was to eventually be able to bind two of these **L1** groups to Ru in cis configuration, occupying four of the six coordination sites around Ru leaving two sites unused. This would project the carboxylates toward the surface allowing for a two-point attachment to TiO_2 layer. The two empty sites could then be filled with various groups such as electron-donating, electron-withdrawing, electron-rich or electron-poor and study the effect of each on the resulting complex as a dye. We also wanted to explore a homoleptic Ru complex with three **L1** groups in which, the fifth and sixth coordination sites of Ru were occupied by a third **L1**. In this case we wouldn't know if the carboxylate on the third unit would bind to the TiO_2 layer unless all of the carboxylates point in the same region space leaving no *trans* relationship between any of the two carboxylates present around the Ru. In this case the geometry of the final dye complex was our interest and obtaining the facial arrangement versus the meridional was our goal. The third point to explore involved the NH groups of

the pyrazoles coordinated to Ru that tend to be somewhat acidic and thereby generating a new species containing anionic ligands.

3.2. Synthesis of **L1**

The optimization of **L1** synthesis was challenging. The ester group is desirable because of the advantageous solubility properties that it confers. However, targeting esterified intermediates and products restrict the kinds of reagents used in the reactions. It is noteworthy that attempting to preserve the ester prevents us from using harsh reagents.

There are three reactions involved in synthesis of **L1**. The first step is the synthesis of **P1** using the presumed Minisci reaction. In this reaction acetyl radicals are generated from paraldehyde in the presence of tert-butoxide radical in acidic medium. The acetyl radical then attacks the electrophilic position two on the protonated methyl isonicotinate to produce the protonated **P1** which is more acidic than protonated methyl isonicotinate and therefore in the presence of only one equivalent of TFA, the thermodynamic equilibrium lies towards deprotonated **P1** and the proton is recycled.

The reaction is not straightforward and the method was specifically perfected for this specific reaction. The exact compound was reported in literature by Ishihara et al. and was never purified. The product was obtained as a brownish oil and was used as is.[24]

This was not an option since **P1** was the first reagent in a multi-step synthesis pathway and its purity played an important role in the following steps. As a matter of fact the purification of the brownish oil was performed in our group by Yasmeen Hameed who isolated the major side product using column chromatography and it proved to be a multi-acetylated isonicotinic acid methyl ester. There were multiple experiments performed to determine that the time of the reaction was an important factor in the extent of this side reaction and limiting the time to strictly two hours, significantly reduces the over acetylation. It was also observed that higher yields were obtained when only one equivalent of TFA was used versus three. It was hypothesized that the use of excess amount of acid could lead to the formation of TFA salt of the product that would be lost in the aqueous phase during the extraction step. We are now able to synthesize **P1** in a highly pure form with a modest yield of 80%. The high level of purity is important for synthesis of **P2**.

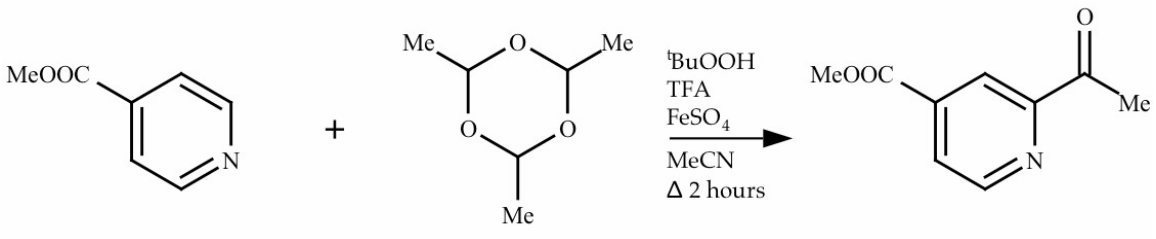

Figure 3.2.1. *The reaction diagram for the synthesis of P1.*

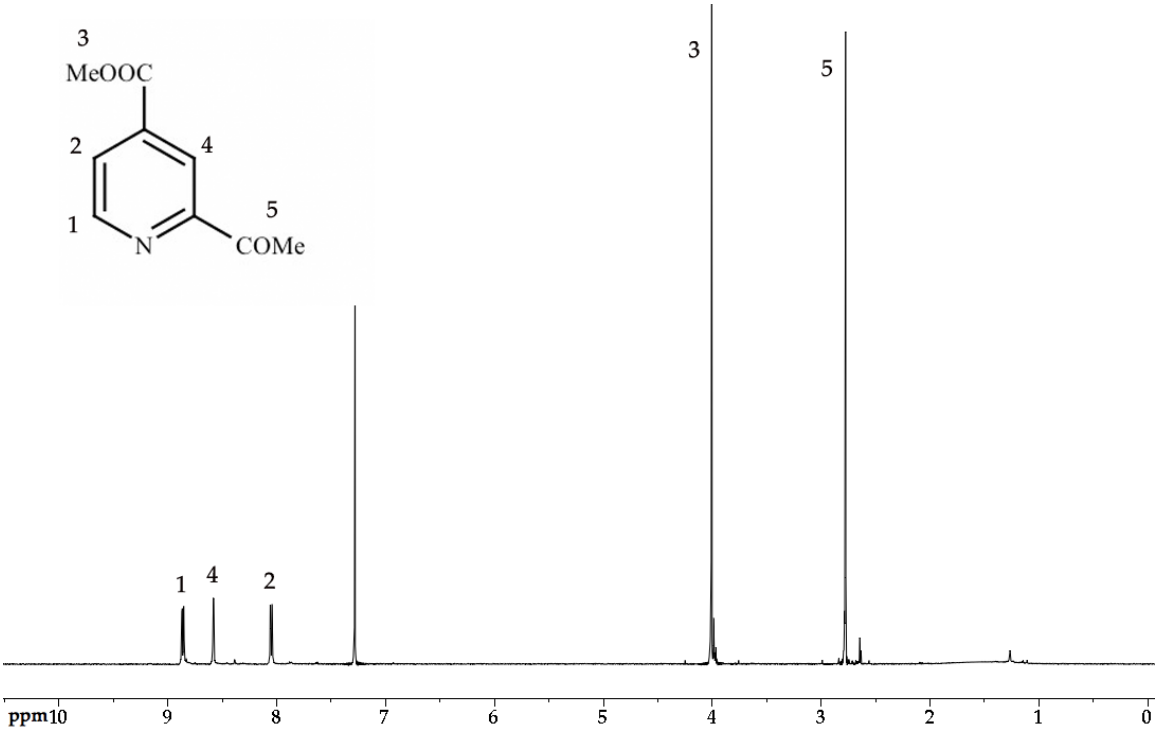

Figure 3.2.2. *The ^{1}H-NMR spectrum of P1 obtained in $CDCl_3$.*

In the second step a novel compound, **P2**, is synthesized. The method[31] was used to synthesize a bispyrazolylpyridine ligand. That molecule does not contain an ester group and the product readily precipitates out of toluene once the reaction has completed. However in our case, most likely due to the presence of the ester group, the product remains dissolved in the solvent. Using somewhat pure **P1** as the starting material and heating the reaction mixture for 17 hours results in a dark-coloured clear mixture with the product remained completely

31 Develay, S.; Blackburn, O.; Thompson, A. L.; Williams, J. A. G. Cyclometalated platinum(II) complexes of pyrazole-based, N=C=N-coordinating, terdentate ligands: the contrasting influence of pyrazolyl and pyridyl rings on luminescence. Inorg. Chem. 2008, 47, 11129-42.

dissolved in the toluene. In the early attempts simply drying off the toluene left a tar-like material that did not give a very clean NMR spectrum. However trituration with chloroform resulted in precipitation of some insoluble material that could be filtered off. Nevertheless the remaining chloroform dissolved material still showed residual impurities on the NMR spectrum. Therefore multiple triturations were required to improve the purity but this resulted in a significant loss of product. At this point simultaneous experiment with the production of **P1** resulted in an improved purity and by using this material in the synthesis of **P2**, we managed to obtain a much purer product without extensive purification through trituration. Once very pure **P1** was used, simply evaporating the toluene product without any triturations with chloroform resulted in a tan-coloured powder in quantitative yield. Upon scaling up the reaction the purity was further improved resulting in a golden powder. This product however was not pure enough for elemental analysis therefore no further characterization was performed.

As it is shown in *Figure 3.2.3*, there are clear changes observed from the spectrum obtained for **P1**. Other than the changes in the chemical shifts, there is the appearance of four new signals. These include two belonging to the alkene

hydrogens observed at 8.03 ppm and 6.48 ppm as well as the two methyl signals belonging to the dimethylamino group at 3.22 ppm and 3.03 ppm.

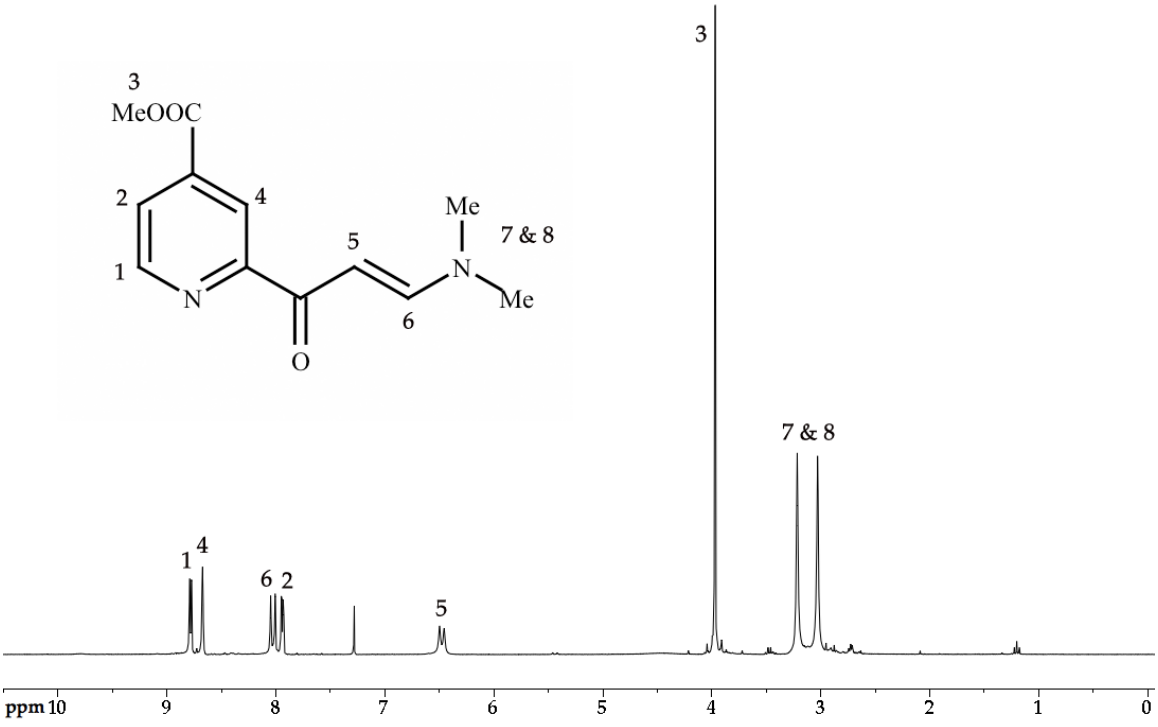

Figure 3.2.3. *The ^{1}H-NMR spectrum of P2 obtained in $CDCl_3$.*

The next step involved converting **P2** to **L1** by treating with hydrazine. The method used required heating **P2** with hydrazine hydrate in methanol at reflux. Under these reaction conditions, some partial hydrolysis of the ester was evident and perhaps inevitable. Increase in the time of the reaction resulted in an increased hydrolysis of the ester, leaving a mixture of products. Along with the hydrolyzed ester side product, it was discovered that over a long time heating at reflux a third side product was also formed, which was not fully characterized but was presumably the hydrazide resulting from the nucleophilic attack of hydrazine on the ester further complicating the situation. It was also attempted to re-esterify the pyrazolylpyridine carboxylic acid to recover the desired product **L1** but this was a long process and proceeded in a very low yield and hence it was an inefficient alternative path.

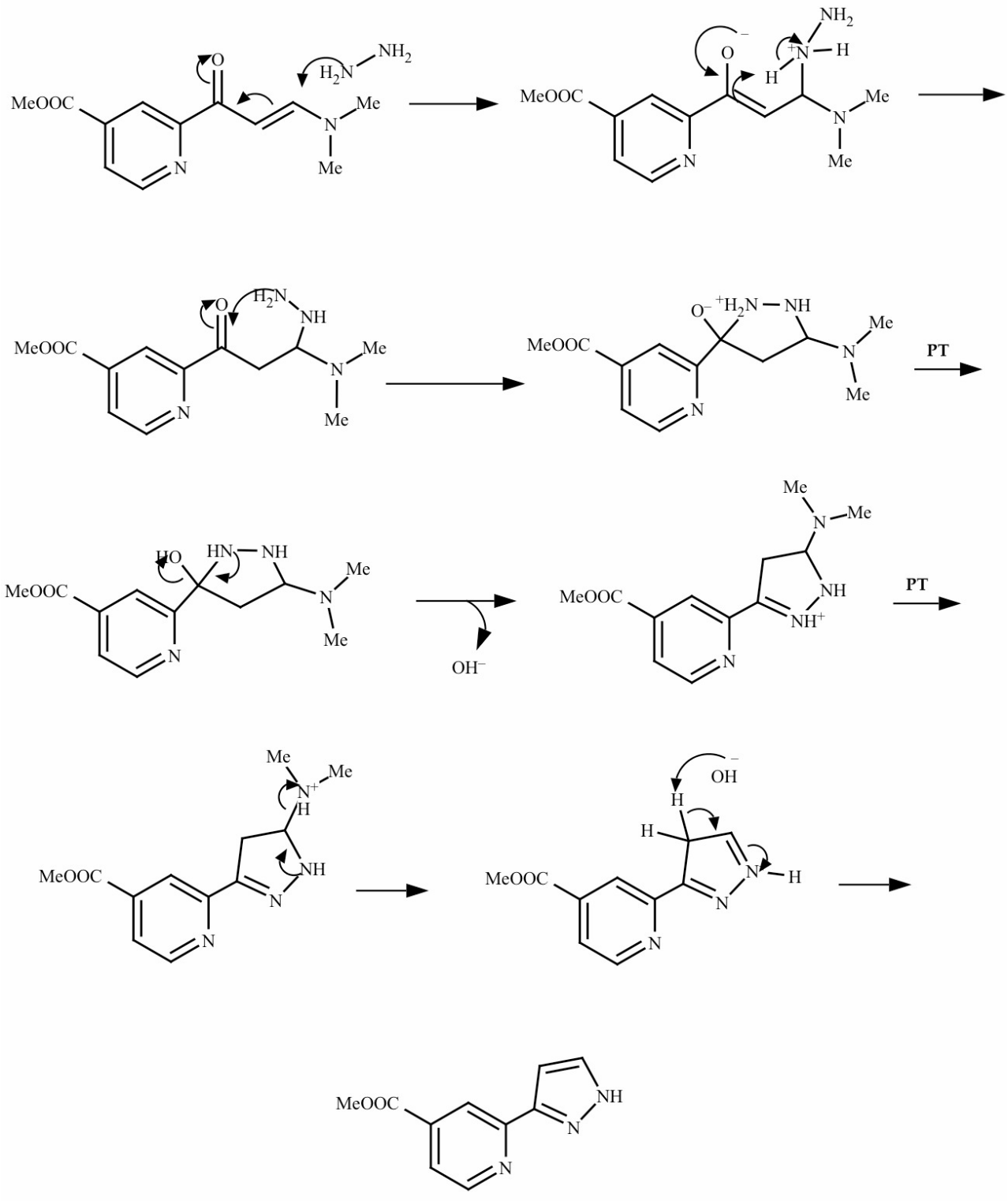

Figure 3.2.4. *The mechanism of L1 synthesis. PT is proton transfer.*

The ^{1}H-NMR spectrum of pure **L1**, shown in *Figure 3.2.5.*, is completely consistent with the expected structure. There are five signals in the aromatic region representing protons belonging to the pyridine and the pyrazole rings and a single peak belonging to the methyl ester at 3.97 ppm. The pyridine doublets are more downfield as expected with the most downfield signal belonging to the proton at position 1 neighbouring the pyridine nitrogen showing a chemical shift of 8.77 ppm. The next peak is a singlet and the only expected singlet on the pyridine ring at position 4 followed by the next doublet belonging to the pyridine ring as well at position 2. The two remaining extremely fine doublets belong to the pyrazole rings hydrogens with the more downfield doublet at 7.70 ppm belonging to position 6 hydrogen being next to the pyrazole nitrogen and finally position 5 proton shows a doublet at 6.91 ppm. The coupling constants provide further information on the interactions of the protons belonging to the same ring system. The J coupling constants of signals 1 and 2 are 5.0 Hz and the J coupling constants of signals 5 and 6 are both 2.1 Hz.

We were unsuccessful in obtaining X-Ray quality crystals for **L1**. Many different solvent combinations mostly chloroform/hexane and chloroform/ether at various ratios were used in attempts carried out at either at room temperature or colder temperatures. We only managed to obtain very fragile and small

crystals therefore no crystal structures are reported for this compound. However, further characterization data for **L1** are provided in the appendix section A of this thesis.

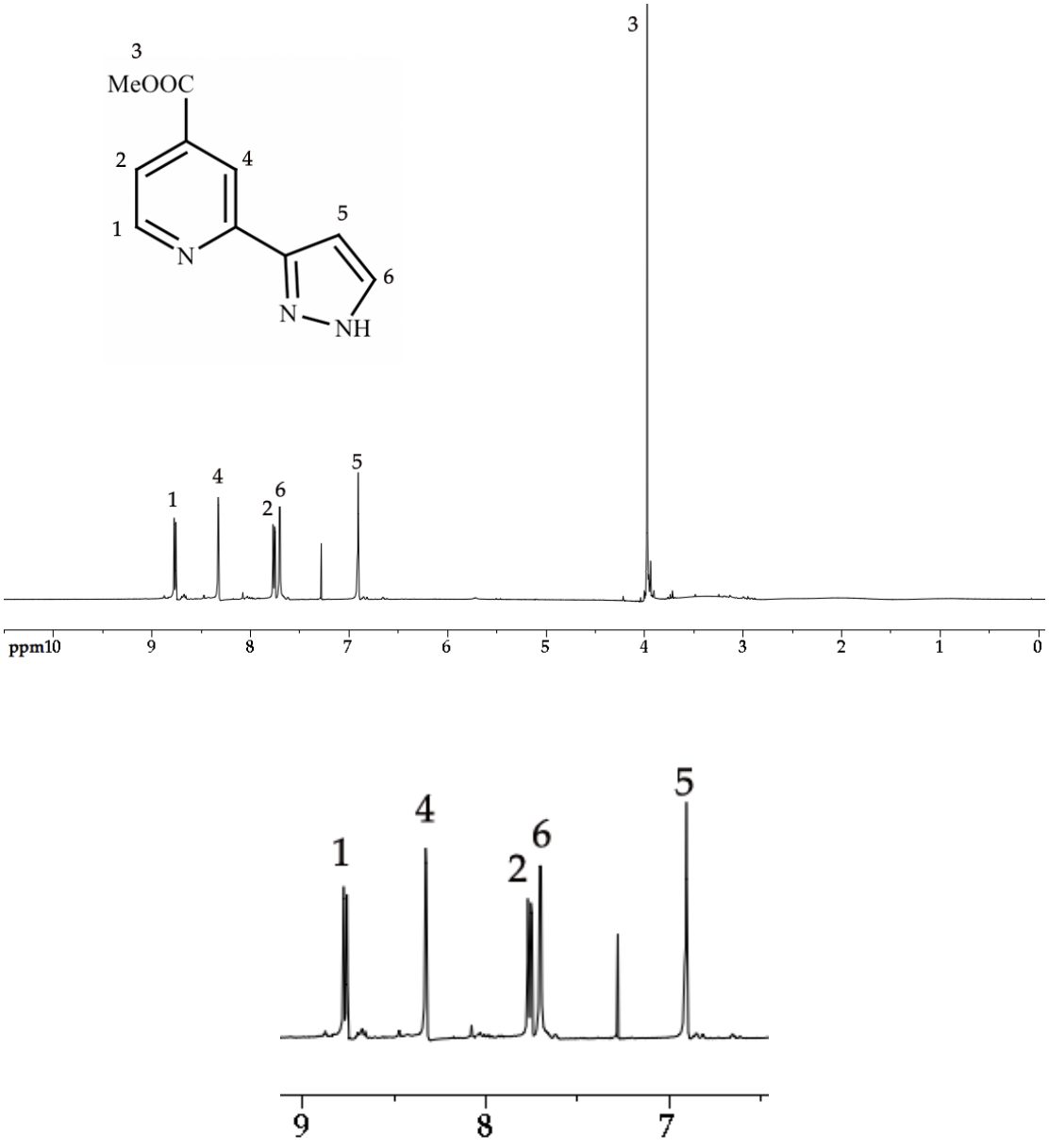

Figure 3.2.5. *The ^{1}H-NMR spectrum of L1 obtained in $CDCl_3$.*

3.3. Design and Synthesis of **L2**

Having **L1** in hand allowed us to incorporate it into a variety of other ligands including **L2**. The tripod design was presumably beneficial in the sense that it would provide a chelation effect positioning three **L1** units around the metal. Upon successful coordination to the metal and hydrolysis of the esters, the resulting octahedral complex would be the facial arrangement and hence the desired Ru complex would be obtained. Complex **T1** also would have been interesting to study in terms of electronics and performance as a dye sensitizer.

The alkylating agent, **P3**, was synthesized by the chlorination of triethanolamine using thionyl chloride in chloroform. This method of preparation was very straight forward and yielded solid white crystals of the product ammonium salt in quantitative yield.

In order to carry on with the reaction to obtain **L2**, a series of model reactions were carried out in order to optimize the reaction conditions before applying them to the precious starting material **L1**. Thus three equivalents of 3,5-dimethylpyrazole treated with one equivalent of **P3** salt on a milli mole scale in dry THF under anhydrous conditions, first at room temperature and then with heating. Samples were collected periodically and quenched with a drop of acetic acid before evaporation of the THF to dryness. However, NMR analysis showed

dominant presence of the starting material and some signs of new peaks that could belong to the new desired product. We switched to dry DMF in order to achieve higher temperatures. This showed some promise, after a few hours of heating a larger sample was transferred to a separatory funnel and submitted to partition between chloroform and water in order to get rid of any residual NaH as well as any inorganic products present. Nevertheless the yield of organic soluble material was negligible although the NMR spectrum showed new signals that were in accordance with the expectations for the desired product.

Since the reaction showed some progress in hot DMF, the same reaction conditions were used with the actual pyrazole compound, **L1**. The reaction mixture turned dark within 15 minutes and some precipitate appeared. After heating for a few hours a sample was collected from the supernatant and the NMR spectrum showed no sign of new signals owing to the product. On the hypothesis that the product was part of the precipitate, a sample was removed from the precipitate and NMR spectrum was obtained in TFA-d. There were some signals observed that were consistent with the expected product, however there were no signals attributable to ester methyl groups as well as some other signals possibly belonging to impurities or intermediate compounds.

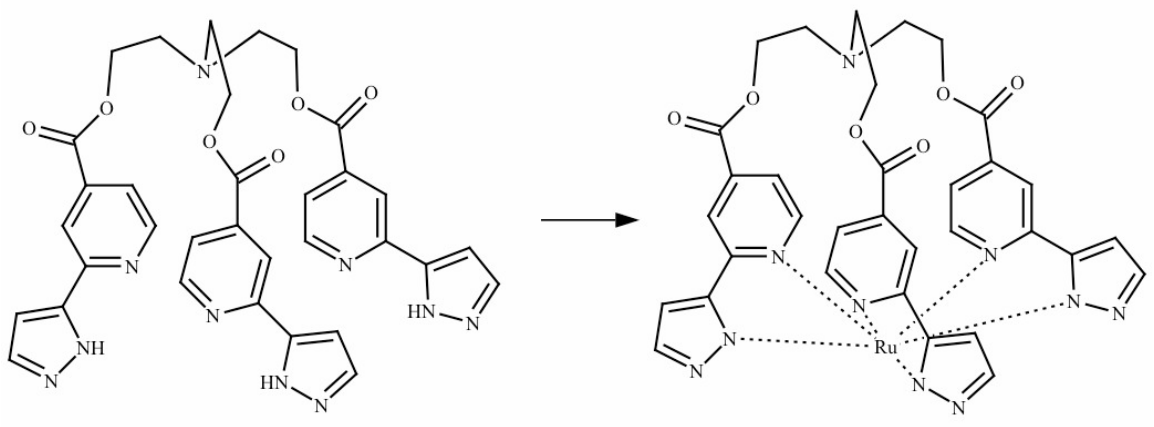

Figure 3.3.1. *The goal molecule of successful trans-esterification shown on the left and the final Ru complex is shown on the right before the hydrolysis of the ester.*

We hypothesized that the ester groups had hydrolyzed through the course of this experiments possibly due to the presence of basic conditions at high temperature and, perhaps involving adventitious water or impure NaH. To be safe we carried out the reaction in DMF at room temperature to verify whether or not we could proceed without hydrolysis. Indeed there was no precipitation at room temperature, however the NMR spectrum of the sample showed one major set of signals belonging to **L1** and small signs of some other product. The reaction was then heated in a water bath in steps, first at 45°C for a few hours and 75°C. Once the temperature was raised to 75°C, similar observation to the previous reaction in hot DMF was observed with tar-like material stuck to the walls of the flask. The mixture was quenched with 2% NH_4Cl solution and extracted with

DCM three times. The DCM extracts were combined and dried and the NMR spectrum showed a mixture of products, again lacking the ester groups signal.

We therefore turned to the trans-esterification pathway in which we heated three equivalents of **L1** with one equivalent of triethanolamine in order to form a tri-ester. This was carried out in MeOH on an NMR scale with heating at 50°C under a stream of air to remove the MeOH and drive away the MeOH released upon the trans-esterification. After the solvent was completely removed, the water bath temperature was increased to 70°C and left there for a few hours. The residue inside the NMR tube was now insoluble in chloroform and therefore DMSO-d6 was used to obtain an NMR spectrum. The spectrum was dominated by the starting material but a small amount of other material that was consistent with the desired product was observed. We repeated this reaction at a larger scale inside a round bottom flask but were not able to obtain the desired material. Next an attempt was made to heat the reaction mixture in an oil bath at ~90°C for 24 hours. There a tar-like residue was formed, that was only soluble in very polar solvents and again the NMR spectrum showed signs of ample starting material. In the absence of solvent using Dean Stark trap to remove the MeOH byproduct, we noticed no formation of the desired product.

3.4. Design and Synthesis of Tridentate Ligands Derived from **L1**

As described in previous section, **L1** has two basic functionalities that can be exploited for synthetic elaboration. The nucleophilic pyrazole presumably allows us to achieve more complex ligands through alkylation reactions. The interest in this, as mentioned earlier, is due to the recent studies that have shown that dyes with highly conjugated π systems show higher stability as well as improved light harvesting capability.[6,7]

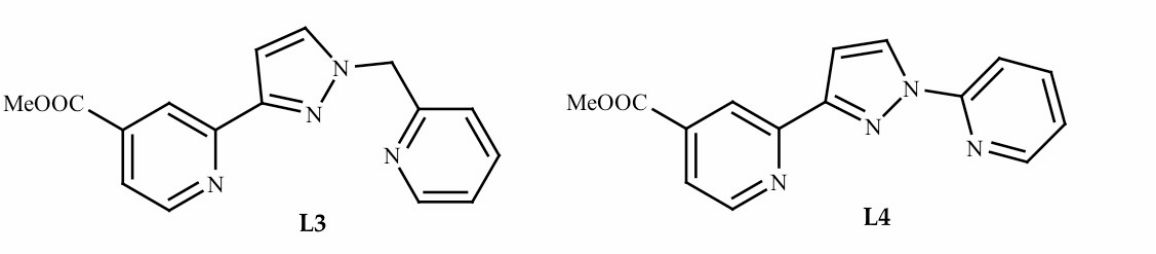

Figure 3.4.1. *Target tridentate analogues of L1.*

Two approaches were followed to transform the bidentate **L1** to a tridentate analogue. One target molecule was **L3** in which a pyridylmethyl is attached and the other is **L4** in which the pyridyl group is directly attached to the pyrazole. The difference anticipated between these two products lies in the bite angle that they would provide Ru. In **L4** the binding is similar to what would be expected in a terpyridine or bipyridine whereas in **L3** the additional pyridine is

not conjugated with the rest of the molecule. **L3** has particular features that are noteworthy. The additional pyridine does not extend the π system therefore it should not significantly alter the electronic features of the ligand, but acts as a mild electron donating group and yet it affords us a tridentate ligand, which has the advantage over bidentates in avoiding geometric isomers in forming a Ru complex.

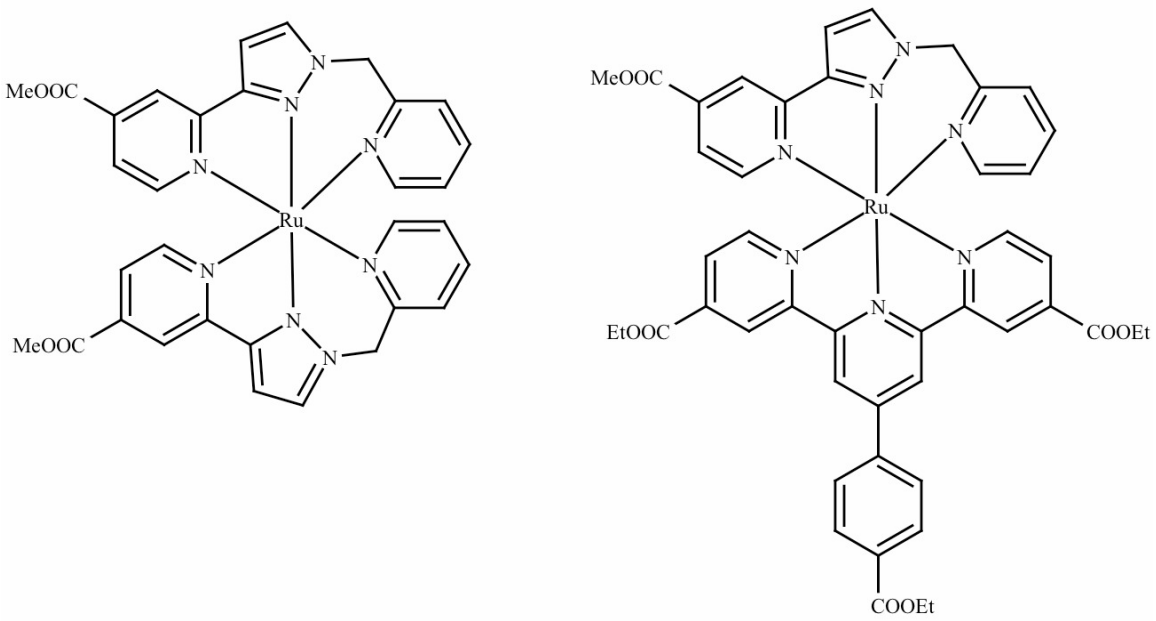

Figure 3.4.2. *The diagram on the left depicts a homoleptic Ru complex with L3 and the one on the right is a depiction of a heteroleptic Ru complex with L3 and L6.*

Figure 3.4.2 shows two examples of bis tridentates. The homoleptic complex ends up containing two ester groups positioned to afford two point binding to TiO_2 surface. The disadvantage of alkylation at this point is that we can no longer change the electronics of the ligand by deprotonation of the pyrazole nitrogen but it should be possible to alter the electronics somewhat through the groupings attached.

Our very first attempt was the use of a simple picolyl grouping. In order to do this we used 2-picolyl chloride hydrochloride salt commercially available following basically the procedure done with the **P3** salt in dry DMF under anhydrous conditions with excess NaH in a 1:1 ratio between **L1** and 2-picolyl chloride. The NMR samples showed many signals that were unexpected and in addition showed loss of the methyl ester signal. Taking a step backwards, we used ethyl iodide to test the alkylation using the same reaction conditions, however the NMR spectrum obtained for this reaction was full of extraneous peaks. To achieve **L4**, we attempted a direct substitution on 2-bromopyridine. Under the same conditions the loss of the methyl signal was observed on the NMR spectrum. In the last attempt we switched away from the NaH towards $Li(TMS)_2N$ again in DMF. This would avoid presence of adventitious water contaminating NaH. This reaction showed a formation of a dark solid but

isolation of the precipitate nor the supernatant quenched with acetic acid showed any sign of the formation of the desired product.

Since the alkylation pathway to substituted pyrazole groups was unsuccessful, we decided to take a step back and treat **P2** with substituted hydrazines. We explored multiple reactions using a number of different substituted hydrazines such as phenyl hydrazine and 2-hydrazinopyridine. The reaction conditions were kept similar as the synthesis of **L1**. In both cases the NMR spectra contained the expected peaks as well as a few extra peaks. The only downside to this reaction pathways was the the ambiguity caused by the phenyl group's unknown site of attachment. Yue Luo had previously worked on substituted pyrazolylpyridines, and the isolation of the "out" isomer versus the "in" isomer was investigated in his research. He was able to isolate the "out" isomer in 77% yield by chelation control using $ZnCl_2$ in the reaction. It was found that without the use of a chelating agent, and performing the condensation reaction with the substituted hydrazine alone, it would lead to the formation of the "in" isomer as the major product.[32]

In our case, $ZnCl_2$ was not ideal due to its solubility in H_2O as well as introduction of moisture to the reaction environment. Hence we performed the

32 Luo, Y.; Potvin, P. G. Chelation-Controlled Regioselectivity in the Synthesis of Substituted Pyrazolylpyridine Ligands. 1. Bidentates. *J. Org. Chem*. 1994, *59*, 1761-5.

2-hydrazinopyridine reaction in the presence of $Fe(NH_4)_2(SO_4)_2$. It was anticipated that iron would act as the chelating agent by coordinating to the pyrazole and pyridine nitrogens allowing for a more controlled reaction towards the production of the "out" isomer as the major product. The NMR sample from the crude in DMSO-d_6 was not conclusive therefore a mini extraction was performed by dissolving the sample in D_2O containing EDTA disodium salt and treating that with $CDCl_3$ inside the NMR tube. Majority of the expected product was observed in the organic layer along with left over starting material. The reaction was further heated to completion, however this was destructive and the product was not obtained.

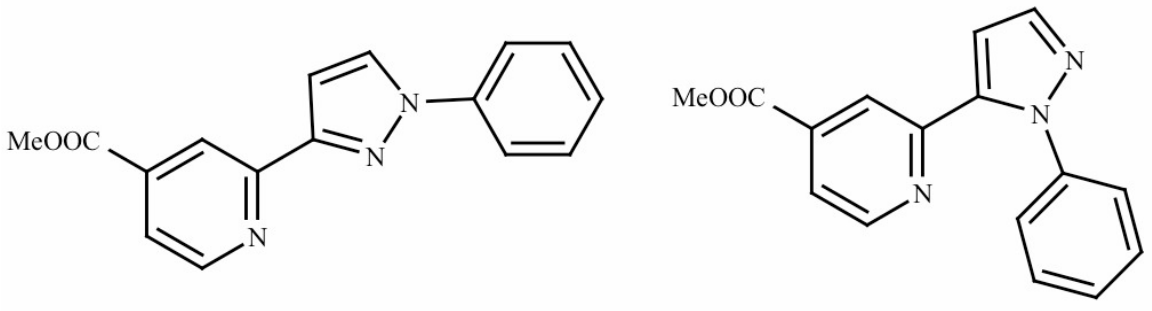

Figure 3.4.3. *The two possible outcomes of reacting P2 with phenyl hydrazine hydrochloride "out" isomer shown on the left and "in" isomer on the right.*

Another compound that was investigated for this purpose was also involved the same reaction using 2-hydroxyethylhydrazine as the starting material. This would lead to the formation of an alcohol substituted pyrazole which upon further alkylation would give a ligand composed of two **L1**'s that were linked through an ether shown in *Figure 3.4.4*. Reacting **P2** with 2-hydroxyethylhydrazine proved unsuccessful yielding similar results as the previous reactions with a large amount of starting material present after long hours of heating.

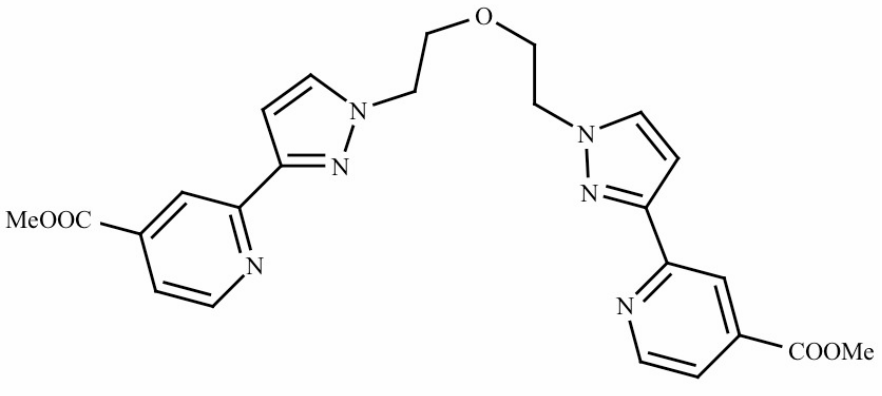

Figure 3.4.4. *Diagram of the target ether ligand composed of two units of L1.*

3.5. Ru Complexes with **L1**

As stated earlier in this thesis, ligand **L1** was designed for the attachment to Ru mimicking the **N3** dye containing two bidentate ligands and two thiocyanate groups. At the same time we were also interested in the homoleptic complex containing three **L1** units as this can be seen to be a mimicry of the **Black Dye** in that there are three pyridine rings and three pyrazole rings that replace the thiocyanates as well as three carboxylate groups.

$RuCl_3 \bullet 3H_2O$ is a good general starting material for these purposes. However there are a few disadvantages to it. It is somewhat hygroscopic making it slightly difficult to work with especially in controlling the stoichiometry on the small scale synthesis. In terms of oxidation state, Ru is at a 3^+ oxidation state and requires a reduction step. This can be achieved either by adding a reducing agent or by the solvent at a high temperature. Lastly abstracting all three chloro groups is difficult, especially the last one. In previous work performed in Potvin lab, it was determined that the addition of $AgBF_4$ helps to facilitate this reaction. The silver ions abstract chlorides causing precipitation of AgCl replacing the chloride ligands with solvent, which are easier to substitute by added ligand. In fact it was determined that this can be done all in one pot, with the desired ligand and $AgBF_4$ added to the solvent in order to get neat homoleptic complexes. The same

Ru starting material and the two equivalents of **L1** without the use of silver can also be used to achieve a dichloro complex. In this case it is necessary to use a reducing solvent such as an alcohol or a reducing agent such as an amine source. Generally it is recognized that the first substitution on to Ru does not involve a loss of a chloride followed by the second substitution that results loss of one chloride and as soon as there are two anionic ligands attached to Ru, the Ru^{3+} oxidation state becomes less stable than Ru^{2+} which at a high temperature a solvent such as an alcohol or a reducing agent such as n-methylmorpholine can be used to reduce the product down to Ru^{2+}. The same results are expected when using $Ru(DMSO)_4Cl_2$ as the starting material, which is already in a Ru^{2+} state so no reduction is required. The dichloro product, in principle can then be converted to a dithiocyanato in an exact imitation of the Grätzel procedure for preparing the **N3** dye. Normally this involves heating the dichloro species with a source of SCN, such as NaSCN in DMF for some time. The reaction can produce some linkage isomers with respect to the SCN binding through nitrogen or sulphur. Some attempts were made to convert the dichloro complex to a dithiocyanato species. However, other work in this lab had discovered that $(Me_3N)_3Ru(SCN)_6$ can be used as the Ru source under more modest temperature conditions and would lead to the thiocyanato Ru complex directly and it was

shown that only a single isomer with all N-linked SCN bound to Ru would be obtained.[33]

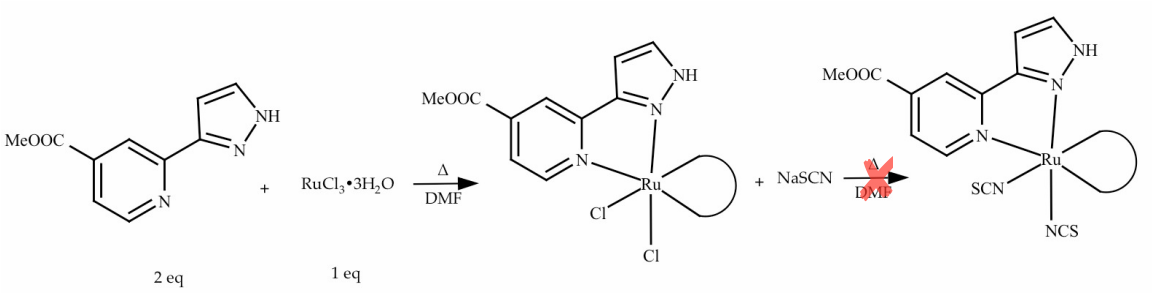

Figure 3.5.1. *Synthesis of the N3 dye analogue using L1 in a two step reaction.*

In our first attempt $RuCl_3 \bullet 3H_2O$ was treated with two equivalents of **L1** in DMF inside a water bath at 100°C for three hours. Intense colour change ensued which suggested complex formation. An NMR sample showed one set of signals but not all of the product would dissolve in the NMR solvent. Therefore we could not be certain that all of the starting material had been consumed. However we pursued this reaction with treating this product with NaSCN in hot DMF overnight following the Grätzel procedure. After 24 hours of heating an NMR sample showed a large number of peaks that were not easily distinguished

33 Luo, Y.; Potvin, P. G. Structural studies on pyrazolylpyridine ligands and complexes. Comparisons between linkage isomers and with 2,2'-bipyridine. *J. Coord. Chem.* 1999, *46*, 319-334.

one from the other. Clearly a reaction had taken place but it did not produce a single product.

The next attempt used $(Me_3N)_3Ru(SCN)_6$ as the Ru source in a standard 1:1 THF/DMF mixture to achieve a modest boiling point in the presence of $^{i}pr_2NH$ as the reducing agent. After 10 hours of heating the reaction mixture had turned black. At this point the excess $^{i}pr_2NH$ and THF were evaporated off and the remaining DMF solution was concentrated down. Precipitate was obtained by dropping the concentrated DMF solution in ether and then it was dissolved in CD_3CN for NMR analysis. However this provided no detectable signals. We suspected that this occurred due to the presence of paramagnetic Ru^{3+} which would rationalize as either a failure at the reduction step from the Ru^{3+} starting material or it could be a result of the deprotonation of the coordinated pyrazole uncoordinated nitrogens, which would then cause **L1** to become anionic and stabilize a Ru^{3+} state. In order to get around this we attempted to reprotonate the pyrazole groups by treating it with HPF_6. This changed the colour of the solution from dark blue which is associated with Ru^{3+} to wine red which is associated with Ru^{2+} species. However the solubility of the PF_6 salt was worse than the original precipitate and once more no signals were observed. TLC also revealed multiple components to this reaction product. Column chromatography was

attempted to isolate the most intensely coloured mobile fractions. The NMR analysis of these fractions however showed no signals what so ever so we concluded that the products of this process were remained in the Ru^{3+} state.

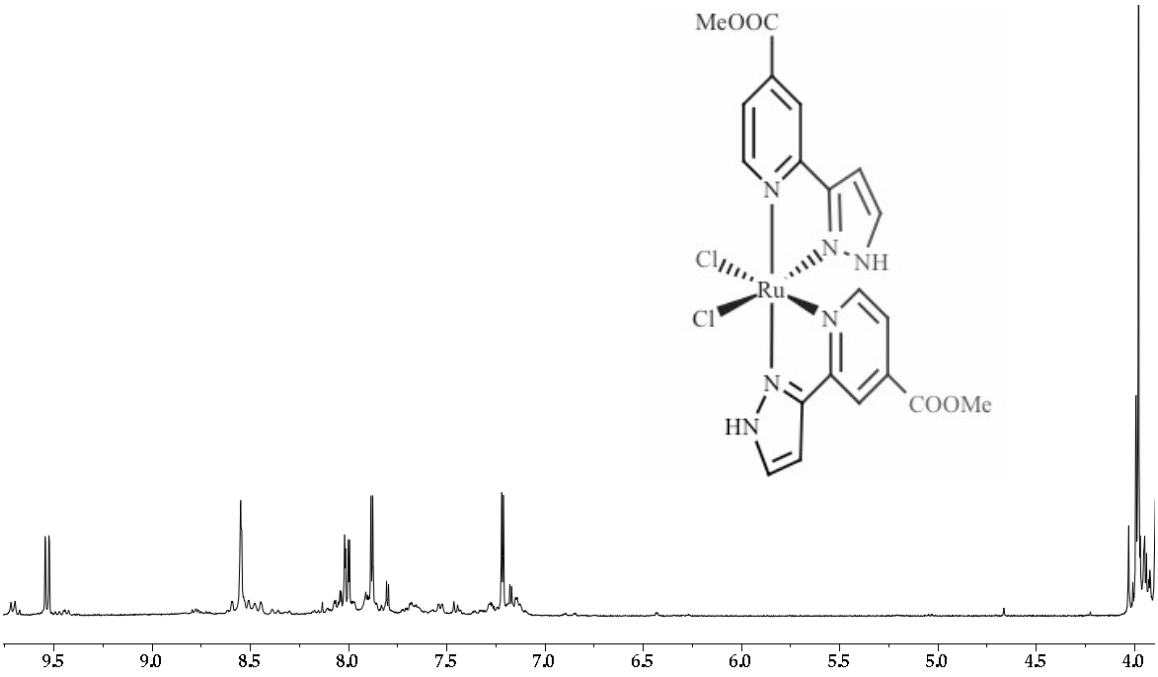

Figure 3.5.2. *The ^{1}H-NMR spectrum of bischloro Ru complex with two L1 groups in CD_3CN.*

In an attempt to avoid the deprotonation of the pyrazole uncoordinated nitrogens, we decided to repeat the same reaction in the absence of $^{i}pr_2NH$ and hoped to achieve reduction of the Ru^{3+} from the solvent alone. DMF is known to decompose to dimethylamine and carbon monoxide at high temperatures. Dimethylamine is then able to act as the reducing agent. However, this was not successful and a Ru^{3+} species was suspected.

Taking a step backward we decided to try and isolate the dichloro Ru complex again using two equivalents of **L1**. Our first attempt at this used $RuCl_3 \bullet 3H_2O$ in DMF in the presence of $^{i}pr_2NH$. However similar observations were made with response to the NMR data. In this case however only one major component was observed on the TLC plate. We then attempted the synthesis of the dichloro complex using $Ru(DMSO)_4Cl_2$ as the Ru source, which as stated earlier is already in Ru^{2+} state. However in all attempts using both NMR and TLC analysis, signs of starting material had been observed when the reaction was carried out in MeOH. When we switched to DMF to achieve a higher temperature, we did see some new major peaks that were consistent with the product but again not all of the sample was soluble in the deuterated solvent and further purification of the product did not seem possible. Unfortunately repeating this process, revealed that the reaction method was not reproducible and we never again were able to achieve the same result for some unknown reason. The same $Ru(DMSO)_4Cl_2$ starting material was again used with two equivalents and also three equivalents of **L1** in two different reactions using 4:1 $MeOH/H_2O$ as the solvent to achieve a higher boiling point than just MeOH to presumably better replace the DMSO ligands. These reactions were monitored

for over a weak and the NMR spectra showed only slight changes in the chemical shifts and many unexpected peaks possibly from intermediate species.

Nevertheless, we decided to convert the only relatively successfully obtained dichloro Ru complex resulting from the irreproducible DMF reaction to the corresponding dithiocyanato complex, the **N3** analogue. This was done again using NaSCN as the SCN source and $AgBF_4$ for facilitating the substitution of DMF. Upon the addition of the silver however, the mixture turned cloudy and some dark material precipitated out, yet we decided to heat the mixture further for a few hours even though it was no longer uniform. We worked up the reaction mixture by filtering off the precipitate. However all the colour associated with the formation of a complex was remained in the precipitate and the supernatant was colourless. The solid was then examined and was found to be completely insoluble and no NMR data could be obtained. We then realized that the $AgBF_4$ may not have been as innocent as expected and the initial precipitate may well have been a silver thiocyanate which would be a very well known process. This time we referred back to an older procedure whereby we perform the abstraction of the chlorides separately from the attachment of the ligand. This process calls for heating the $RuCl_3 \bullet 3H_2O$ with three equivalents of $AgBF_4$ in acetone in order to cause formation of the silver chloride which is insoluble in

acetone and to replace the chlorines with acetone solvate ligands which would leave the Ru dissolved in the acetone. The silver chloride is then filtered off and the acetone is replaced with DMF followed by the addition of the desired ligand. This is done to prevent any silver from coming into contact with either SCN or the ligand. However when the ligand was added and the reaction mixture was allowed to heat overnight, silver sediment was still observed at the bottom of the flask and the same results were obtained as before.

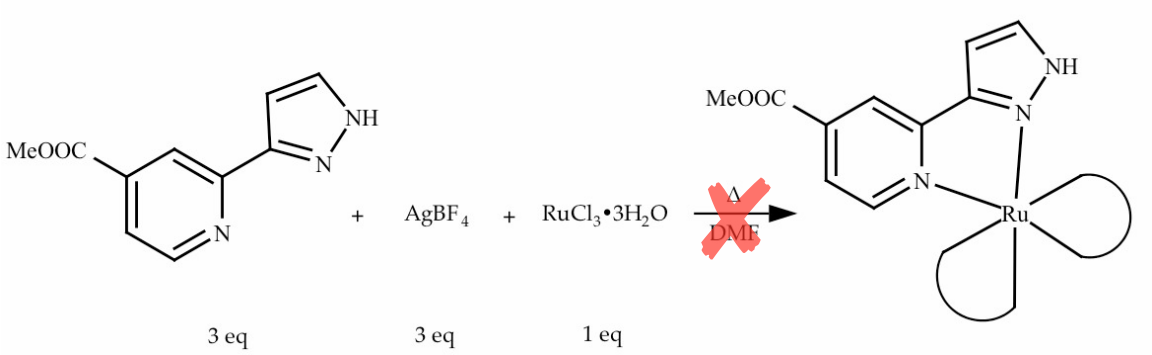

Figure 3.5.3. *Synthesis of homoleptic Ru complex in the presence of silver.*

At this point we grew suspicious about the fact that perhaps silver was interfering with the reaction so we simply treated one equivalent of **L1** with one equivalent of $AgBF_4$ in DMF in the absence of any Ru source. Indeed the reaction turned very dark within one hour of heating suggesting that a reaction had indeed taken place. Removing a solvent left a sample that was used for NMR

analysis and it was clear that there was no free **L1** left, as there was absolutely nothing soluble in the deutorated chloroform.

Another attempt involved the synthesis of a homoleptic Ru complex with three equivalents of **L1** using $RuCl_3 \bullet 3H_2O$ in DMF. During the first multiple attempts we still were unaware of the effect $AgBF_4$ had and therefore it was used in the same pot as the other starting material. Clearly no positive results were obtained from these reactions. The NMR samples obtained continuously showed a range of peaks lead us to believe that we had mixture of isomers and left over starting material. Due to these observations, the reaction was repeated multiple times and NMR samples were obtained at 24, 48 and 72 hours. Each time the silver precipitate was filtered out using celite and a precipitate was then obtained from concentrated DMF solution by adding to water. The precipitate was then isolated and it was found to be quite soluble in CD_3CN. However the only detectable signals observed were belonging to **L1**.

Once we realized that $AgBF_4$ was interfering with this process, we decided to revert back to the original procedures from older literature using very high boiling ethylene glycol as the solvent. This was done by boiling three equivalents of **L1** with one equivalent of $RuCl_3 \bullet 3H_2O$ in ethylene glycol. Samples were removed after 24, 48 and 72 hours of heating. The NMR spectra obtained were

not clear and TLC analysis showed no significant separation between products. Postulating that perhaps the reaction had gone on for too long, we worked up a separate reaction after 24 hours. This time the reaction mixture was slowly added to saturated NH_4PF_6 solution converting it to a PF_6 salt. The NMR spectrum obtained from the solid shows clear signals belonging to a new complex having lost the methoxy ester peak due to the trans-esterification that had occurred with ethylene glycol. The yield for this reaction after the isolation procedure was only about 24%. The NMR spectrum for this product is shown in *Figure 3.5.4*.

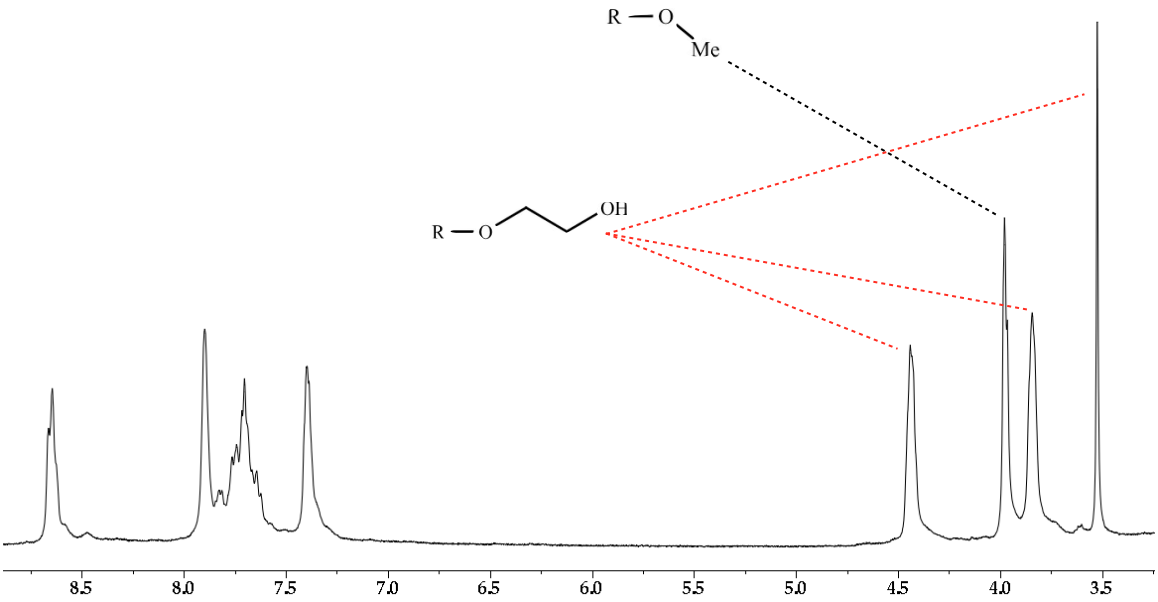

Figure 3.5.4. *The ^{1}H-NMR spectrum of the homoleptic Ru complex PF_6 salt obtained from the ethylene glycol reaction in CD_3CN.*

As the last attempt we used guidance from Yue Luo's thesis, and tried heating in EtOH instead of MeOH since it was clear that boiling point of MeOH was simply not hot enough to push the reaction forward. There was a downside of trans-esterification, but we decided that it was a minimal issue and could be dealt with once the ligands were coordinated to Ru. After heating a 3:1 mixture of **L1** to $RuCl_3 \bullet 3H_2O$ for three days, there seemed to be no sign of starting material by NMR. The crude product was then redissolved in anhydrous methanol followed by the addition of a small amount of acetyl chloride to generate HCl in situ. This was then set to heat at reflux overnight, after which the reaction mixture was cooled, concentrated to small volume and then added to concentrated solution of aqueous NH_4PF_6. The precipitate was collected and left to dry at room temperature. A sample was removed and dissolved in CD_3CN for NMR analysis. The NMR spectrum was very clean, showing one set of signals in the aromatic region with only one methyl ester signal without the presence of the ethyl ester, showing that the trans-esterification was successful. The yield of the reaction at 0.1 mmol scale was 69% and this was increased to 79% upon scaling up to 0.5 mmol.

In conclusion the only really successful reaction was this latest one with $RuCl_3 \bullet 3H_2O$, three equivalents of **L1** in EtOH to achieve the homoleptic

complex, which seems to facilitate substitution and also allow for the reduction of Ru^{3+} to Ru^{2+}. All the attempts to obtain dichloro and dithiocyanato Ru complexes with **L1** failed.

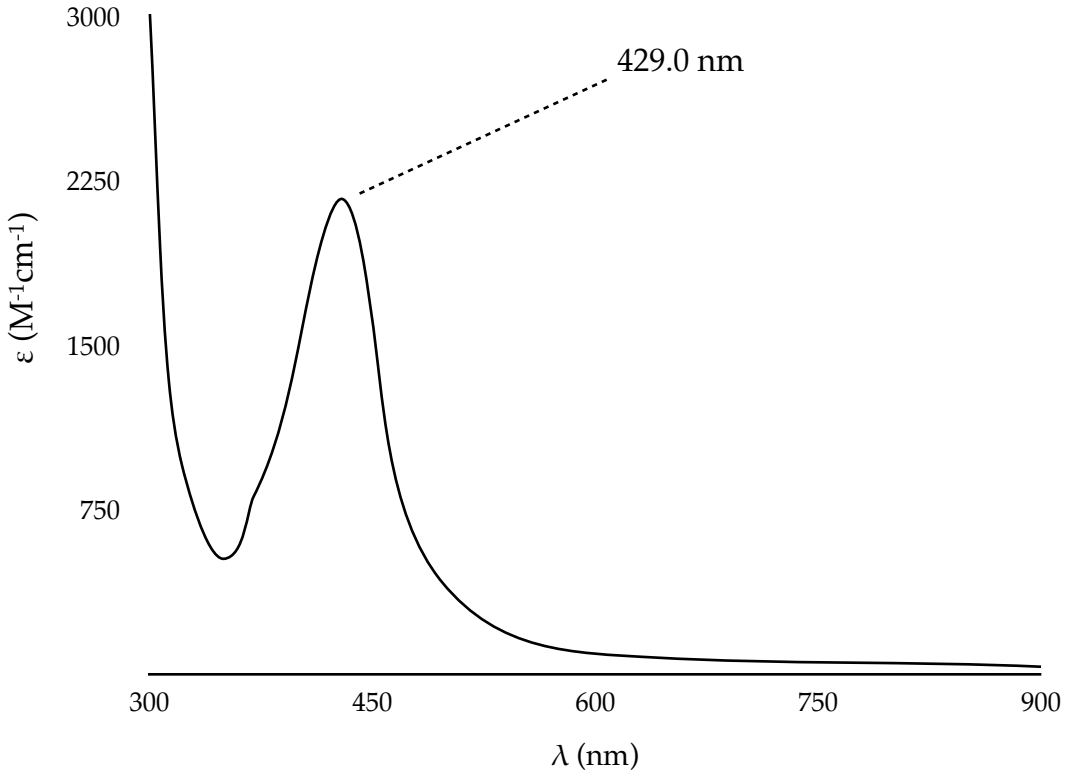

Figure 3.5.5. *UV-Visible spectrum of $Ru(L1)_3(PF_6)_2$ in MeCN solution*

The UV-Visible spectrum of $Ru(L1)_3(PF_6)_2$ is shown in *Figure 3.5.5*. A sharp peak is observed at 429 nm due to the MLCT transitions, which appears to be typical of homoleptic complexes with bidentate ligands. The reported absorption

due to the MLCT transitions by Lam et al.[34] is at 400 nm. This shows that the substituted methyl esters have affected the electronics towards a more red shifted MLCT band. They also have reported that upon deprotonation of the pyrazoles' uncoordinated nitrogens the MLCT band was further shifted to 430 nm, which gives us the ability to further shift the MLCT band if necessary.

The mass spectrum obtained for the $Ru(L1)_3(PF_6)_2$ complex shows clear presence of Ru complex with three ligands either at a doubly charged (shown in *Figure 3.5.6*) or a single charge state. The isotopic distribution for the complex is consistent with the calculated pattern using IsoPro, mass spectral isotopic distribution simulator.

34 Lam, M. H. W.; Cheung, S. T. C.; Fung, K.; Wong, W. Synthesis and X-ray Crystal Structure of a Triple-Stranded Helical Supramolecular Complex Formed between Tris(3-(pyridin-2-yl)pyrazole)ruthenium(II) and Copper(I). *Inorg. Chem.* 1997, *36*, 4618-4619.

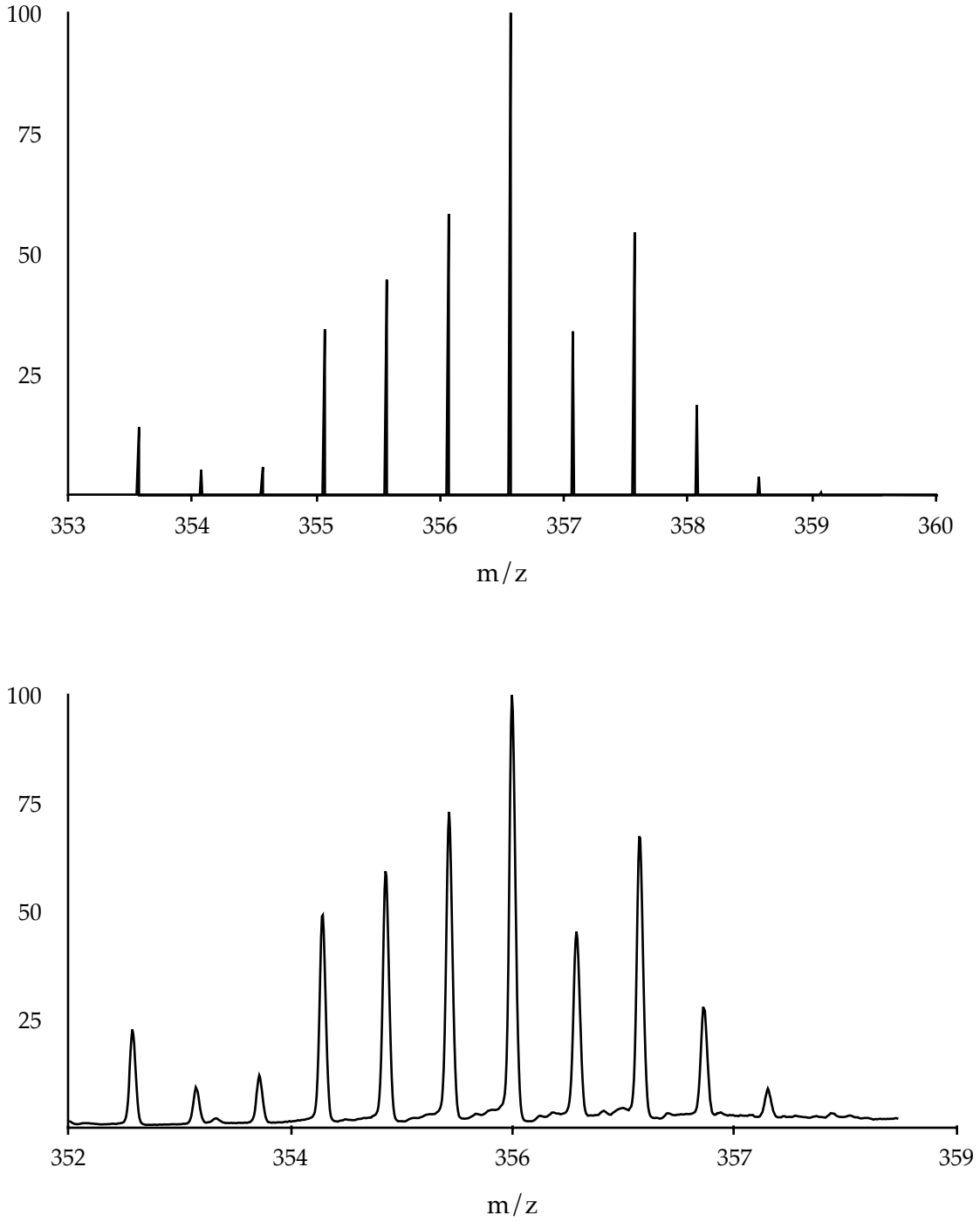

Figure 3.5.6. *The predicted (top) and the actual mass spectrum (bottom) of the doubly charged* $Ru(L1)_3$.

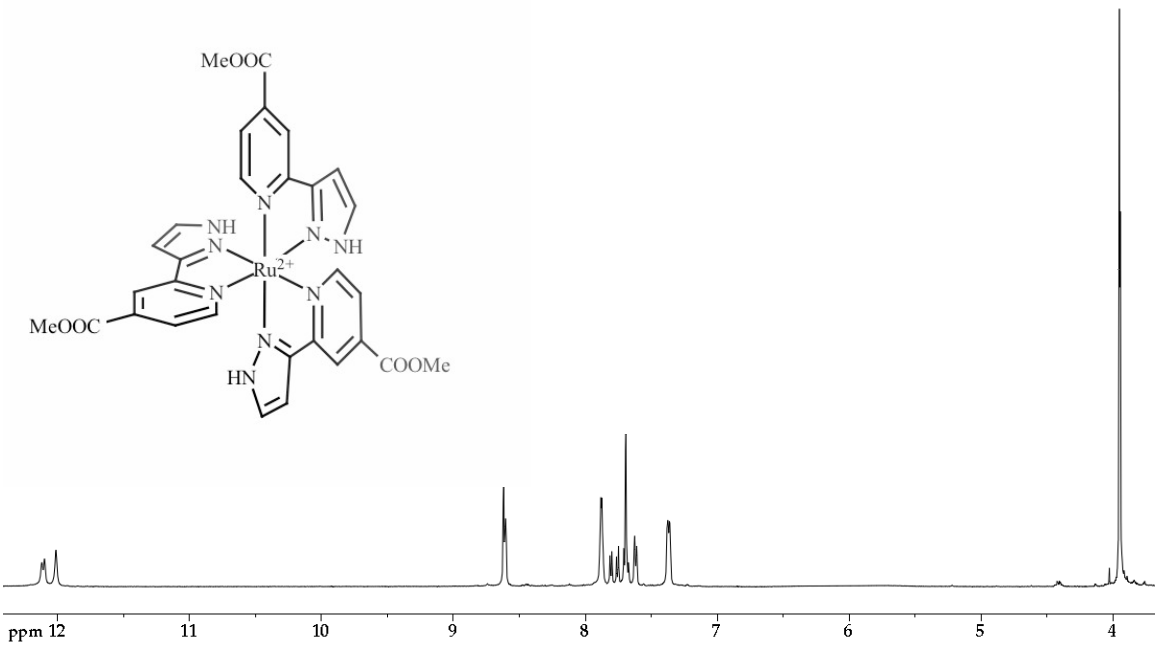

Figure 3.5.7. *The ^{1}H-NMR spectrum of the mixture of fac and mer isomers of the homoleptic Ru complex PF_6 salt in CD_3CN.*

With respect to the homoleptic species, we recognized early that two isomers could be obtained in fact the literature provides precedent for that. Michael Ward recently published a procedure for isolating the *fac* and *mer* isomers from such species using Cu^+ to precipitate out the *fac* isomer and leaving behind mostly the *mer* isomer.[35] In the paper mentioned earlier by Lam, they also explored the same coordination and actually had a look at the crystal structure. The Cu^+ forms an interesting adduct of three coppers binding to pyrazole

35 Metherell, A. J.; Cullen, W.; Stephenson, A.; Hunter, C. A.; Ward, M. D. Fac and mer isomers of Ru(II) tris(pyrazolylpyridine) complexes as models for the vertices of coordination cages: structural characterisation and hydrogen-bonding characteristics. *Dalton Trans.* 2014, *43*, 71-84.

nitrogens of two *fac* Ru complexes forming a cage structure.[36] The issue remaining for us was which Cu^{+} species to use but also appears that Cu^{2+} species can also be used in the presence of a reducing agent. Given that our Ru product was in the form of PF_6 salt instead of the ClO_4 salt, we decided that we needed $CuPF_6$ as our Cu source. To do this we treated $Cu(OAc)_2$ instead of Cu_2O with HPF_6 in MeCN obtaining white crystals of the $Cu(MeCN)_4PF_6$ complex.[37] The Cu complex was then boiled with the Ru complex in MeOH in the presence of TEA to deprotonate the pyrazole nitrogens not coordinated to Ru and facilitate the attachment of Cu to these nitrogens. We carried on by using about 5 equivalents of the Cu with respect to the initial Ru complex in a large excess. Upon addition, the solution turned muddy and a precipitate formed. The mixture was left to heat at reflux for about 8 hours and the precipitate was then filtered off from the mixture. However, it appeared that all of the colour of the reaction mixture came out of the solution in the precipitate, leaving no Ru complex in the solution. It was therefore evident that the separation of the two isomers was not achieved.

---

36 Lam, M. H. W.; Cheung, S. T. C.; Fung, K.; Wong, W. Synthesis and X-ray Crystal Structure of a Triple-Stranded Helical Supramolecular Complex Formed between Tris(3-(pyridin-2-yl)pyrazole)ruthenium(II) and Copper(I). *Inorg. Chem.* 1997, *36*, 4618-4619.

37 Kubas, G. J. Tetrakis(acetonitrile)copper(1+) hexafluorophosphate(1-). *Inorg. Synth.* 1990, *28*, 68-70.

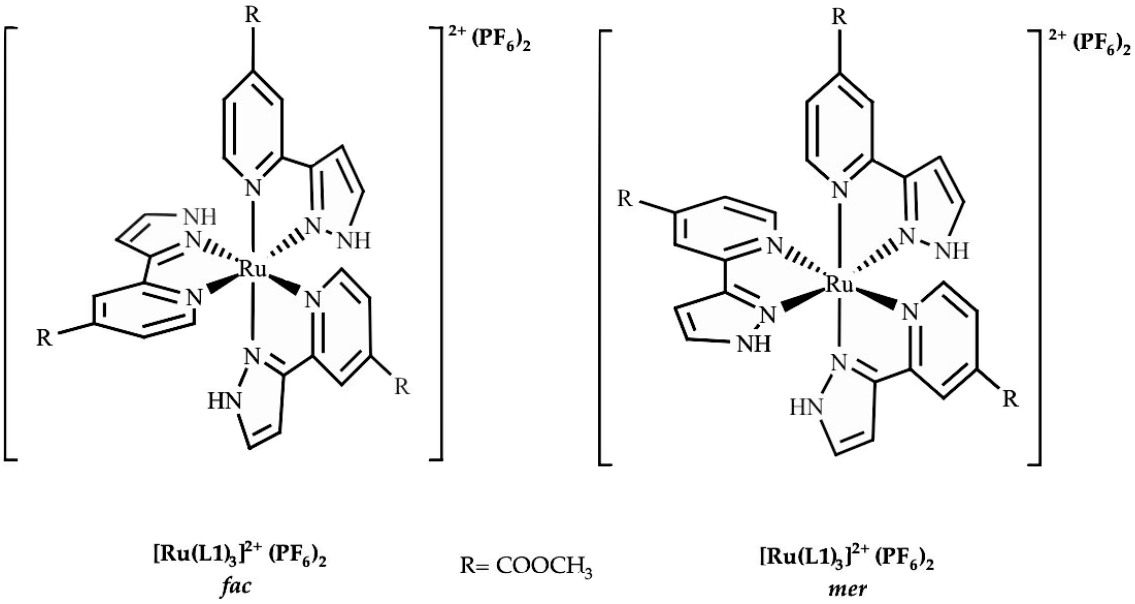

Figure 3.5.8. *The fac and mer isomers of the homoleptic Ru complex PF_6 salt.*

While working with Ru complexes synthesis of other complexes were also explored. Fe being in the same group as Ru also has the capability of forming the same kinds of octahedral complexes with such ligands. Fe is the most abundant metal on earth making it also much cheaper than Ru and it would be much more favourable in large scale industrial production setting. It is somewhat smaller than Ru and suffers from a much faster ligand exchange rates, which makes it difficult to use in order to prepare heteroleptic complexes.

One attempt was to prepare a homoleptic Fe complex using three equivalents of **L1** and $(NH_4)_2Fe(SO_4)_2$ which provides Fe in the required oxidation state. After precipitation as the PF_6 salt, the solid had a requisite intense red colour but NMR analysis was inconclusive because the peaks were all very broad. MS analysis did not reveal the presence of the required mass. This product however was also treated with $Cu(MeCN)_4PF_6$ to produce a possible cage-like structure by boiling the two reagents in MeOH in the presence of excess TEA. This produced an olive green precipitate as required but it was insoluble in all solvents tested.

A brief exploration of Al was also made in order to prepare an analogue of 8-hydroxyquinoline complex forming a photosensitive Al complex. This was completely unsuccessful with no reaction taking place at all.

3.6. Synthesis of Other Bidentate and Tridentate Ligands

Terpyridine ligands have shown to be effective ligands for the purpose of DSSC's. **Black Dye** as one of the most efficient dyes to date is a Ru complex with a terpyridine and three thiocyanate groups. Many different terpyridine ligands have been synthesized in Potvin lab[38] throughout the years and the most recent one that we have developed here involves a terpyridine with three carboxyl groups.

To prepare a terpyridine carboxylate salt, **L5**, we used two different methods one of which developed by Hanan, proved to be a more successful pathway for this particular terpyridine. Generally for ease of handling and better solubility the carboxylate salt is converted to an ester through simple esterification process using concentrated sulphuric acid in dry methanol. This was always easily achieved with one or two carboxyl groups but in this case, it proved to be a tedious process. Another reaction pathway that was explored involved using TFA and heating for 24 hours. However the yield was so low that rendered the process useless.

An attempt was made to use **L5** as a potassium salt to try an mimic the structure of the **Black Dye**, it was combined with $(Me_4N)_3Ru(SCN)_6$ in a 1:1

38 Stublla, A.; Potvin, P. G. Ruthenium(II) Complexes of Carboxylated Terpyridines and Dipyrazinylpyridines. Eur. J. Inorg. Chem. 2010, 3040-3050.

DMF/THF. A few drops of TFA were used to protonate the carboxyl groups and solubilize it in the solution. After 5 hours of heating a sample was obtained to check for completion. The NMR spectrum showed very small peaks in the aromatic region and therefore Ru^{3+} species was suspected. A few drops of $^{i}pr_2NH$ were added to the NMR tube to induce reduction of the Ru complex but it was unsuccessful. The crude reaction mixture was split into two equal amounts and heated at different temperatures to reduce the Ru complex while obtaining the optimal reaction conditions for it. This however was not successful and the complex remained as Ru^{3+}.

The main goal for **L6** was to combine it with one of the tridentate ligands derived from **L1** to generate a heteroleptic Ru complex. Unfortunately the synthesis of the the tridentate ligands from **L1** were unsuccessful and therefore this goal was never achieved.

The synthesis of **L7** and **L8** were exploratory work in order to obtain insight on the nucleophilicity of pyrazole nitrogen for the alkylation in conditions were the alkylating agent contains a heterocycle using our setting. Both reactions were carried out under anhydrous conditions using NaH as base in dry DMF. 2,4-Dimethylpyrazole was used as the nucleophile and 2-bromopyridine for **L8** and 2-picolyl chloride for **L7** were the alkylating agents

used in each reaction. In the case of **L8** the results from the NMR sample was promising, showing chemical shifts on the major peaks in the aromatic region and the presence of the methyl groups. However, after workup the methyl signals disappeared. The possible explanation for this is the attack of a hydroxy group in place of the pyrazole and leading to production of 2-hydroxypyridine instead. Meanwhile **L7** was never obtained. The same reaction was then carried out for **L8** and this time $Li(TMS)_2N$ was used as the base. The use of this base proved to be useful since the expected product was formed, however some starting 2,4-dimethylpyrazole remained unused. The final attempt made to make this pathway work was the use of Cs_2CO_3 as the base which also failed and no product was obtained.

Chapter Four: Conclusion and Future Work

In this thesis the successful synthesis of ligand **L1** is introduced through steps of developing the starting material **P1** and the pathway that yields the purest product and at the highest yield followed by the detailed reaction pathway of the intermediate compound **P2**. The thesis then focuses on multiple reactions performed on **L1** in order to develop tridentate ligands and all the exploratory work that was done to achieve the ultimate reaction conditions. Further analytical data is provided for **L1** in the appendix section A of this thesis.

The exploration of **L1** in complex formation with Ru is also explained in detail including all the failed attempts using various Ru starting materials or other reagents that were involved and finally the complete synthesis pathway of the only successful Ru complex with **L1** is reported in detail. ^{1}H-NMR, ^{13}C-NMR, COSY, HSQC and HMBC data is provided in the appendix section B.

Other exploratory work performed with **L1** as well as complex formation with other metals such as Fe and Al are also discussed here but the attempts were unsuccessful.

References

1. Hoffert, M. I., Caldeira, K., Jain, A. K., Haites, E. F., Harvey, L. D. D., Potter, S. D., Wuebbles, D. J. 1998. Energy implications of future stabilization of atmospheric CO2 content. Nature (London), 395(6705), 881-884.
2. Bredehoeft, G. 2014. (No. #DOE/EIA-0383(2014)). USA: US Energy Information Administration.
3. Rogelj, J., McCollum, D. L., Reisinger, A., Meinshausen, M., & Riahi, K. 2013. Probabilistic cost estimates for climate change mitigation. Nature, 493(7430), 79-83.
4. Williams 1960. "Becquerel Photovoltaic Effect in Binary Compounds". The Journal of Chemical Physics 32 (5): 1505–1514. Bibcode:1960JChPh..32.1505W.
5. Ponnampalam, Dino. DSSC – Transforming A Solar Cell. Energy Trend: Solar. 2011-12-02. <http://www.energytrend.com/DSSC_20111202>. Access Date: 2012-03-30.
6. Gerischer, H.; Michel-Beyerle, M.; Rebentrost, F.; Tributsch, H. Sensitization of charge injection into semiconductors with large band gap. Electrochim. Acta 1968, 13, 1509-15.
7. O'Regan, B.; Graetzel, M. A low-cost, high-efficiency solar cell based on dye-sensitized colloidal titanium dioxide films. Nature (London) 1991, 353, 737-40.

8. Sekar, N.; Gehlot, V. Y. Metal complex dyes for dye-sensitized solar cells: recent developments. Resonance 2010, 15, 819-831.
9. Hara, Kohjiro, and Hironori Arakawa. "Dye-Sensitized Solar Cells".John Wiley & Sons Ltd , 2003. 663-700. Print.
10. Barbe, C. J.; Arendse, F.; Comte, P.; Jirousek, M.; Lenzmann, F.; Shklover, V.; Gratzel, M. Nanocrystalline titanium oxide electrodes for photovoltaic applications. J Am Ceram Soc 1997, 80, 3157-3171.
11. Holliman, P. J.; Mohsen, M.; Connell, A.; Davies, M. L. et al. Ultra-fast co-sensitization and tri-sensitization of dye-sensitized solar cells with N719, SQ1 and triarylamine dyes. J. Mater. Chem. 2012, 22, 13318-13327.
12. Polo, A. S.; Itokazu, M. K.; Murakami Iha, N. Y. Metal complex sensitizers in dye-sensitized solar cells. Coord. Chem. Rev. 2004, 248, 1343-1361.
13. Ferrere, S. New photosensitizers based upon Fe(L)2(CN)2] and Fe(L)3] (L = substituted 2,2'-bipyridine): yields for the photosensitization of TiO2 and effects on the band selectivity. Chem. Mater. 2000, 12, 1083-1089.
14. Altobello, S.; Argazzi, R.; Caramori, S.; Contado, C.; Da Fre, S.; Rubino, P.; Chone, C.; Larramona, G.; Bignozzi, C. A. Sensitization of Nanocrystalline TiO2 with Black Absorbers Based on Os and Ru Polypyridine Complexes. J. Am. Chem. Soc. 2005, 127, 15342-15343.

15. Ning, Z.; Zhang, Q.; Wu, W.; Tian, H. Novel iridium complex with carboxyl pyridyl ligand for dye-sensitized solar cells: High fluorescence intensity, high electron injection efficiency? J. Organomet. Chem. 2009, 694, 2705-2711.
16. Feldt, S. M.; Gibson, E. A.; Gabrielsson, E.; Sun, L.; Boschloo, G.; Hagfeldt, A. Design of Organic Dyes and Cobalt Polypyridine Redox Mediators for High-Efficiency Dye-Sensitized Solar Cells. J. Am. Chem. Soc. 2010, 132, 16714-16724.
17. Yella, A.; Lee, H.; Tsao, H. N.; Yi, C.; Chandiran, A. K.; Nazeeruddin, M. K.; Diau, E. W.; Yeh, C.; Zakeeruddin, S. M.; Graetzel, M. Porphyrin-Sensitized Solar Cells with Cobalt (II/III)-Based Redox Electrolyte Exceed 12% Efficiency. Science (Washington, DC, U. S.) 2011, 334, 629-634.
18. B. O'Regan, M. Grätzel, Nature 335 (1991) 737; (b) M. Grätzel, Nature 414 (2001) 338–344.
19. Anderson, P. A.; Strouse, G. F.; Treadway, J. A.; Keene, F. R.; Meyer, T. J. Black MLCT Absorbers. Inorg. Chem. 1994, 33, 3863-4.
20. Nazeeruddin, M. K.; Pechy, P.; Renouard, T.; Zakeeruddin, S. M.; Humphry-Baker, R.; Comte, P.; Liska, P.; Cevey, L.; Costa, E.; Shklover, V.; Spiccia, L.; Deacon, G. B.; Bignozzi, C. A.; Gratzel, M. Engineering of efficient

panchromatic sensitizers for nanocrystalline TiO(2)-based solar cells. J. Am. Chem. Soc. 2001, 123, 1613-24.

21. Wang, S.; Wu, K.; Ghadiri, E.; et al. Engineering of thiocyanate-free Ru(II) sensitizers for high efficiency dye-sensitized solar cells. Chem. Sci., 2013,4, 2423-2433.
22. Ozawa, H.; Shimizu, R.; Arakawa, H. Significant improvement in the conversion efficiency of black-dye-based dye-sensitized solar cells by cosensitization with organic dye. RSC Adv. 2012, 2, 3198-3200.
23. Kiyoshi, D.; Robson, P. and Berlinguette, C.; Cycloruthenated sensitizers: improving the dye-sensitized solar cell with classical inorganic chemistry principles. Dalton Trans., 2012, 41, 7814.
24. Ishihara, M.; Tsuneya, T.; Shiga, M.; Kawashima, S.; Yamagishi, K.; Yoshida, F.; Sato, H.; Uneyama, K. New pyridine derivatives and basic components in spearmint oil (Mentha gentilis f. cardiaca) and peppermint oil (Mentha piperita). J. Agric. Food Chem. 1992, 40, 1647-55.
25. Develay, S.; Blackburn, O.; Thompson, A. L.; Williams, J. A. G. Cyclometalated platinum(II) complexes of pyrazole-based, N=C=N-coordinating, terdentate ligands: the contrasting influence of pyrazolyl and pyridyl rings on luminescence. Inorg. Chem. 2008, 47, 11129-42.

26. Wilson, E.; Tishler, M. Nitrogen mustards. J. Am. Chem. Soc. 1951, 73, 3635-41.

27. Vougioukalakis, G. C.; Stergiopoulos, T.; Kantonis, G.; Kontos, A. G.; Papadopoulos, K.; Stublla, A.; Potvin, P. G.; Falaras, P. Terpyridine- and 2,6-dipyrazinylpyridine-coordinated ruthenium(II) complexes: Synthesis, characterization and application in TiO2-based dye-sensitized solar cells. J. Photochem. Photobiol. , A 2010, 214, 22-32.

28. Cooke, M. W.; Wang, J.; Theobald, I.; Hanan, G. S. Convenient one-pot procedures for the synthesis of 2,2':6',2''-terpyridine. Synth. Commun. 2006, 36, 1721-1726.

29. Duprez, V.; Krebs, F. C. New carboxy-functionalized terpyridines as precursors for zwitterionic ruthenium complexes for polymer-based solar cells. Tetrahedron Lett. 2006, 47, 3785-3789.

30. Kiyoshi, D.; Robson, P. and Berlinguette, C.; Cycloruthenated sensitizers: improving the dye-sensitized solar cell with classical inorganic chemistry principles. Dalton Trans., 2012, 41, 7814.

31. Develay, S.; Blackburn, O.; Thompson, A. L.; Williams, J. A. G. Cyclometalated platinum(II) complexes of pyrazole-based, N=C=N-coordinating, terdentate ligands: the contrasting influence of pyrazolyl and pyridyl rings on luminescence. Inorg. Chem. 2008, 47, 11129-42.

32. Luo, Y.; Potvin, P. G. Chelation-Controlled Regioselectivity in the Synthesis of Substituted Pyrazolylpyridine Ligands. 1. Bidentates. J. Org. Chem. 1994, 59, 1761-5.

33. Luo, Y.; Potvin, P. G. Structural studies on pyrazolylpyridine ligands and complexes. Comparisons between linkage isomers and with 2,2'-bipyridine. J. Coord. Chem. 1999, 46, 319-334.

34. Lam, M. H. W.; Cheung, S. T. C.; Fung, K.; Wong, W. Synthesis and X-ray Crystal Structure of a Triple-Stranded Helical Supramolecular Complex Formed between Tris(3-(pyridin-2-yl)pyrazole)ruthenium(II) and Copper(I). Inorg. Chem. 1997, 36, 4618-4619.

35. Metherell, A. J.; Cullen, W.; Stephenson, A.; Hunter, C. A.; Ward, M. D. Fac and mer isomers of Ru(II) tris(pyrazolylpyridine) complexes as models for the vertices of coordination cages: structural characterisation and hydrogen-bonding characteristics. Dalton Trans. 2014, 43, 71-84.

36. Lam, M. H. W.; Cheung, S. T. C.; Fung, K.; Wong, W. Synthesis and X-ray Crystal Structure of a Triple-Stranded Helical Supramolecular Complex Formed between Tris(3-(pyridin-2-yl)pyrazole)ruthenium(II) and Copper(I). Inorg. Chem. 1997, 36, 4618-4619.

37. Kubas, G. J. Tetrakis(acetonitrile)copper(1+) hexafluorophosphate(1-). Inorg. Synth. 1990, 28, 68-70.

38. Stublla, A.; Potvin, P. G. Ruthenium(II) Complexes of Carboxylated Terpyridines and Dipyrazinylpyridines. Eur. J. Inorg. Chem. 2010, 3040-3050.

Appendices

Appendix A

^{13}C-NMR spectrum of L1 in $CDCl_3$

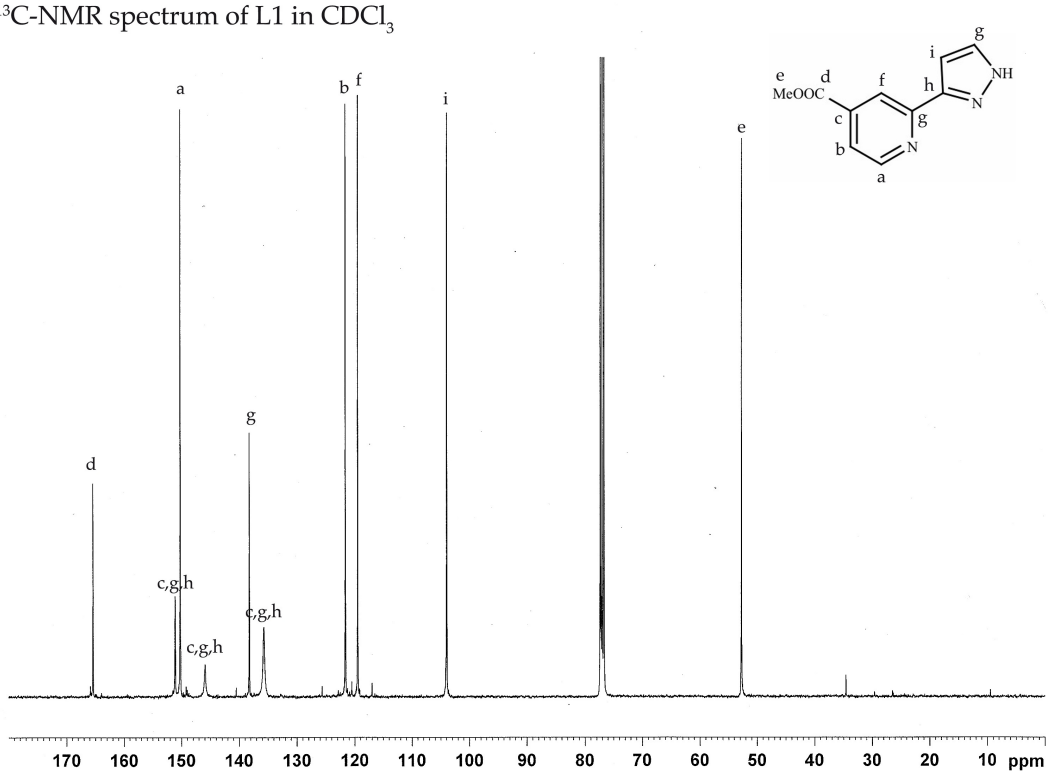

^{1}H-NMR spectrum of L1 in CD_3CN

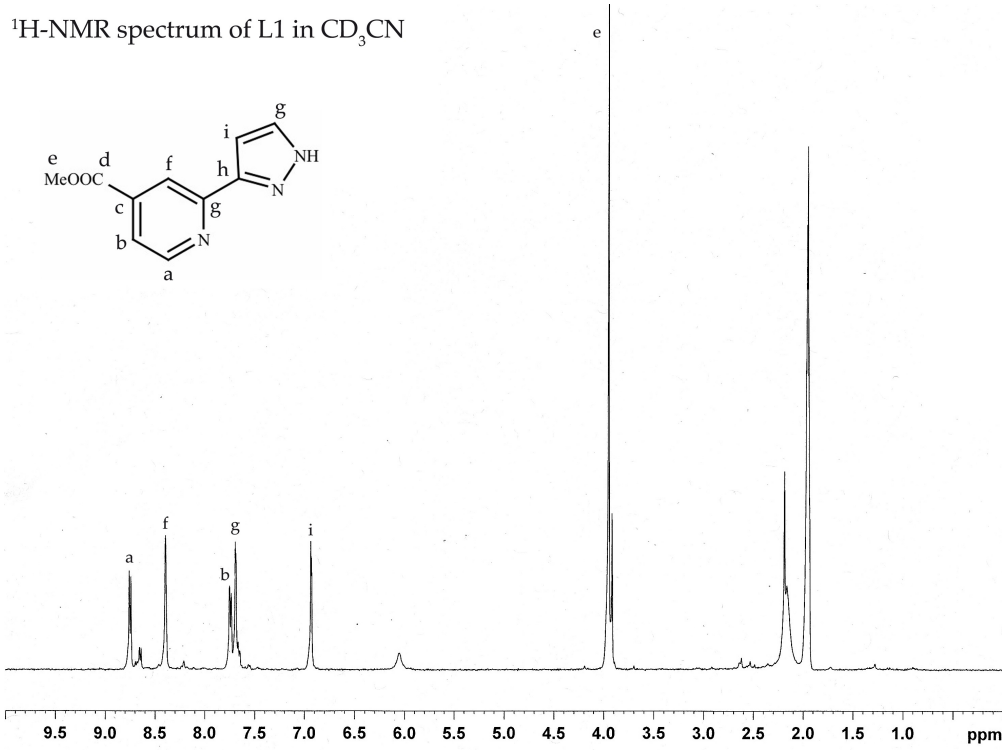

Appendix A

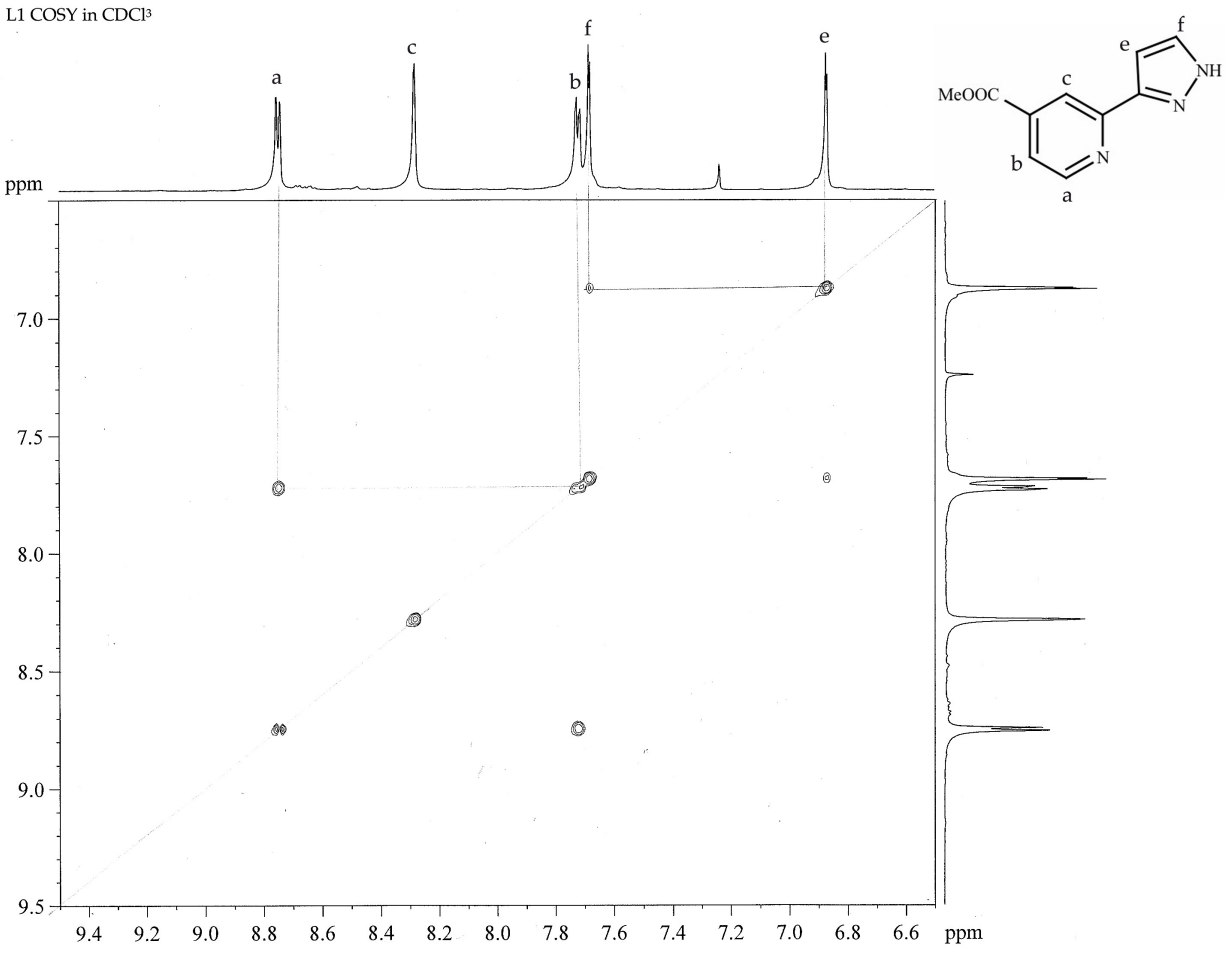
L1 COSY in CDCl3
a
c
b
f
e
ppm
7.0
7.5
8.0
8.5
9.0
9.5
9.4
9.2
9.0
8.8
8.6
8.4
8.2
8.0
7.8
7.6
7.4
7.2
7.0
6.8
6.6
ppm
MeOOC
N
NH
N

Appendix A

L1 HSQC in $CDCl_3$

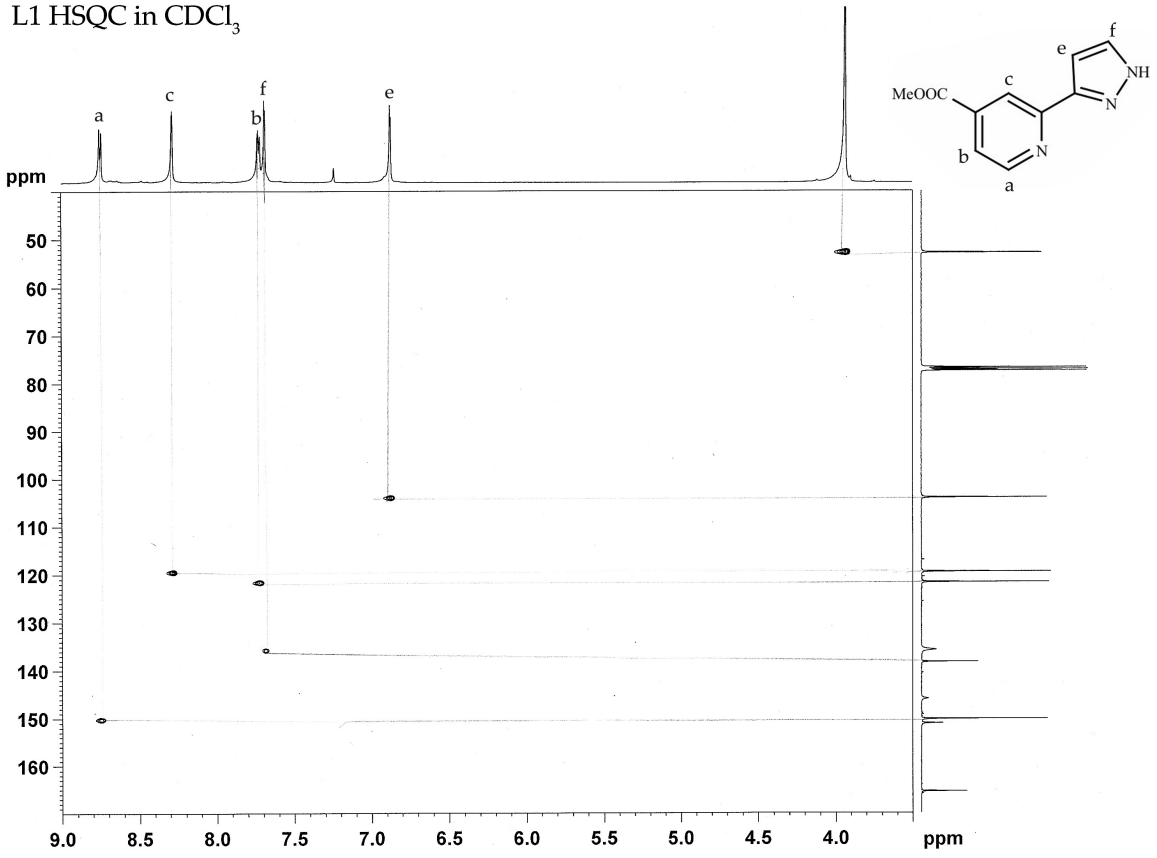

Appendix B

COSY 2-D spectrum using reference ^{1}H-NMR spectra in CD_3CN

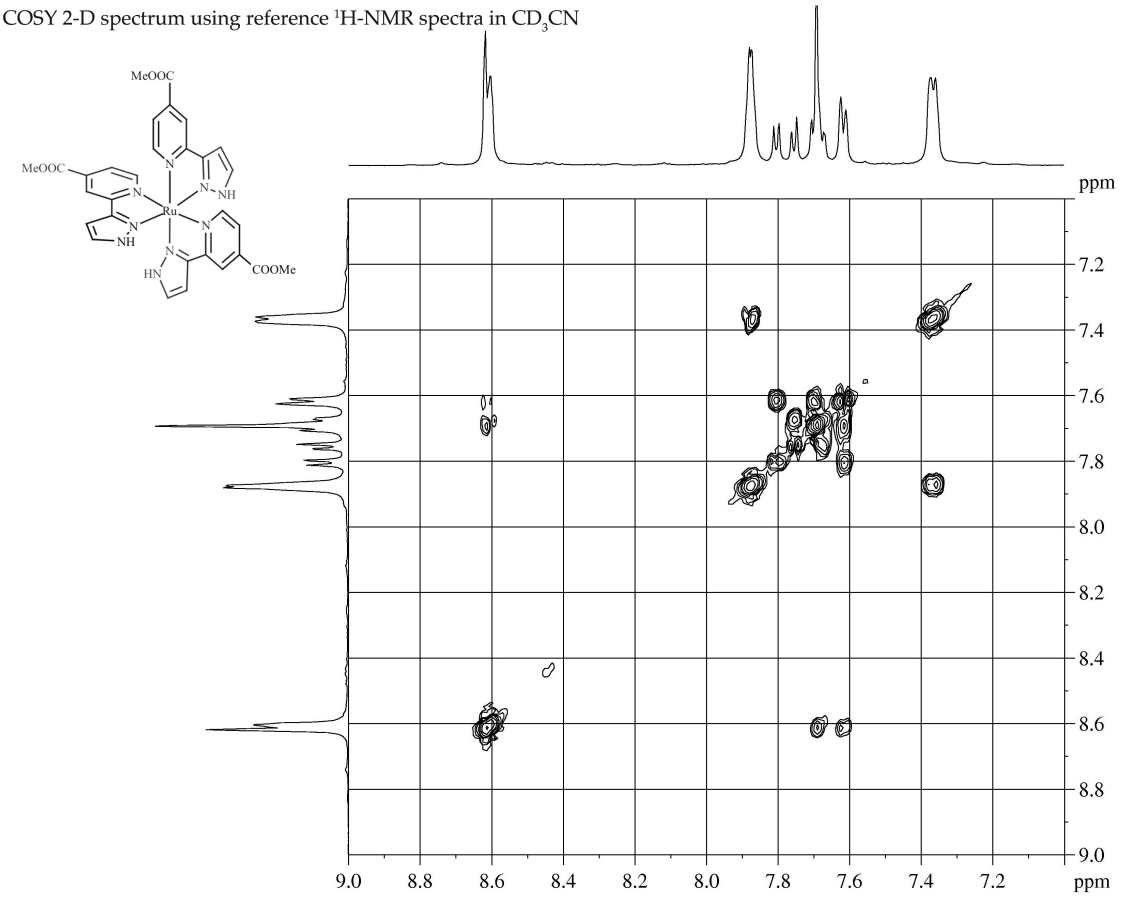

Appendix B

COSY 2-D spectrum using reference ^{1}H-NMR spectra in CD_3CN

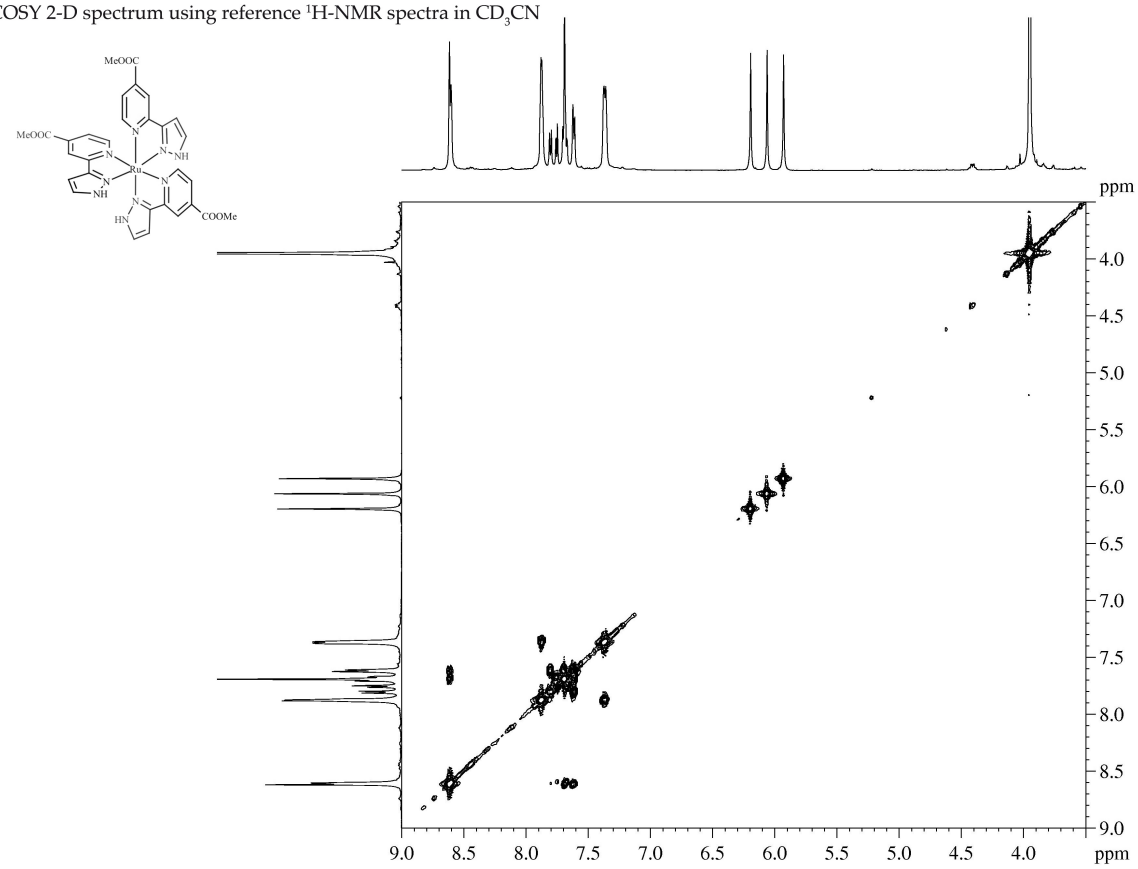

Appendix B

HSQC 2-D spectrum using reference ^{1}H-NMR spectrum (top)
DEPT spectrum (left) in CD_3CN

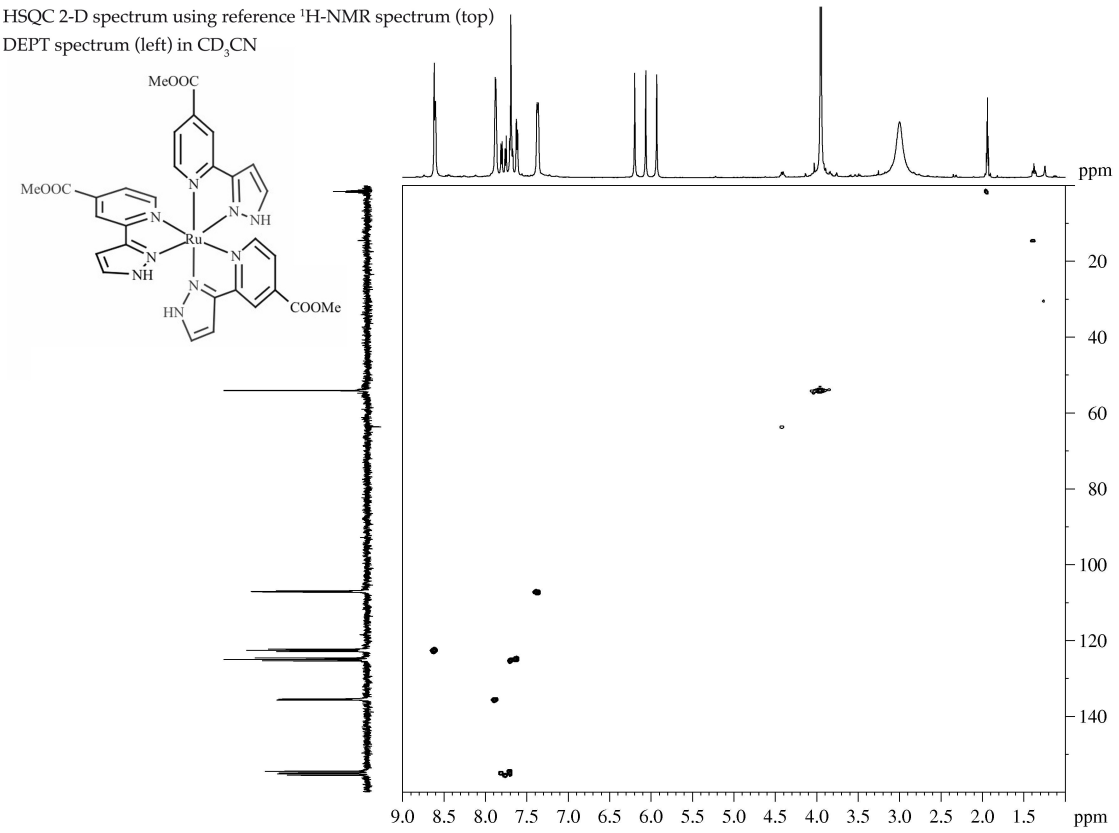

Appendix B

HSQC 2-D spectrum using reference ^{1}H-NMR spectrum (top) DEPT spectrum (left) in CD_3CN

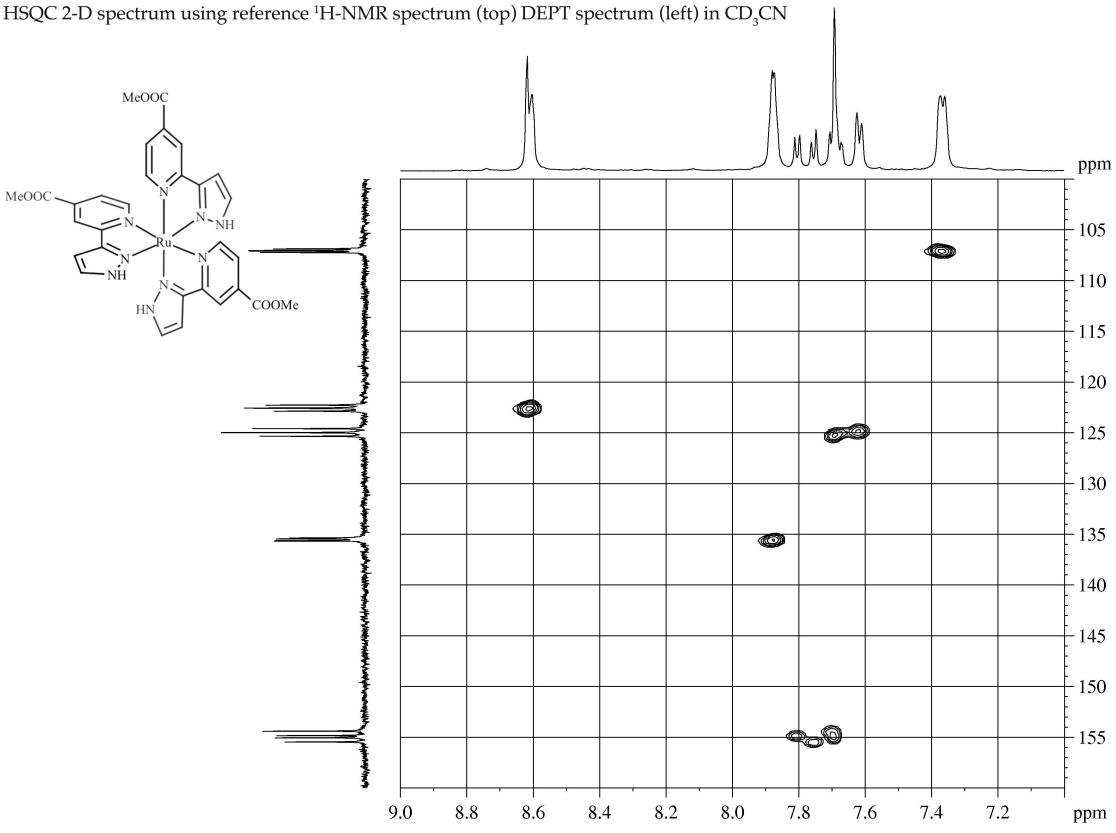

Appendix B

HMBC 2-D spectrum using reference ^{1}H-NMR spectrum (top)
^{13}C spectrum (left) in CD_3CN

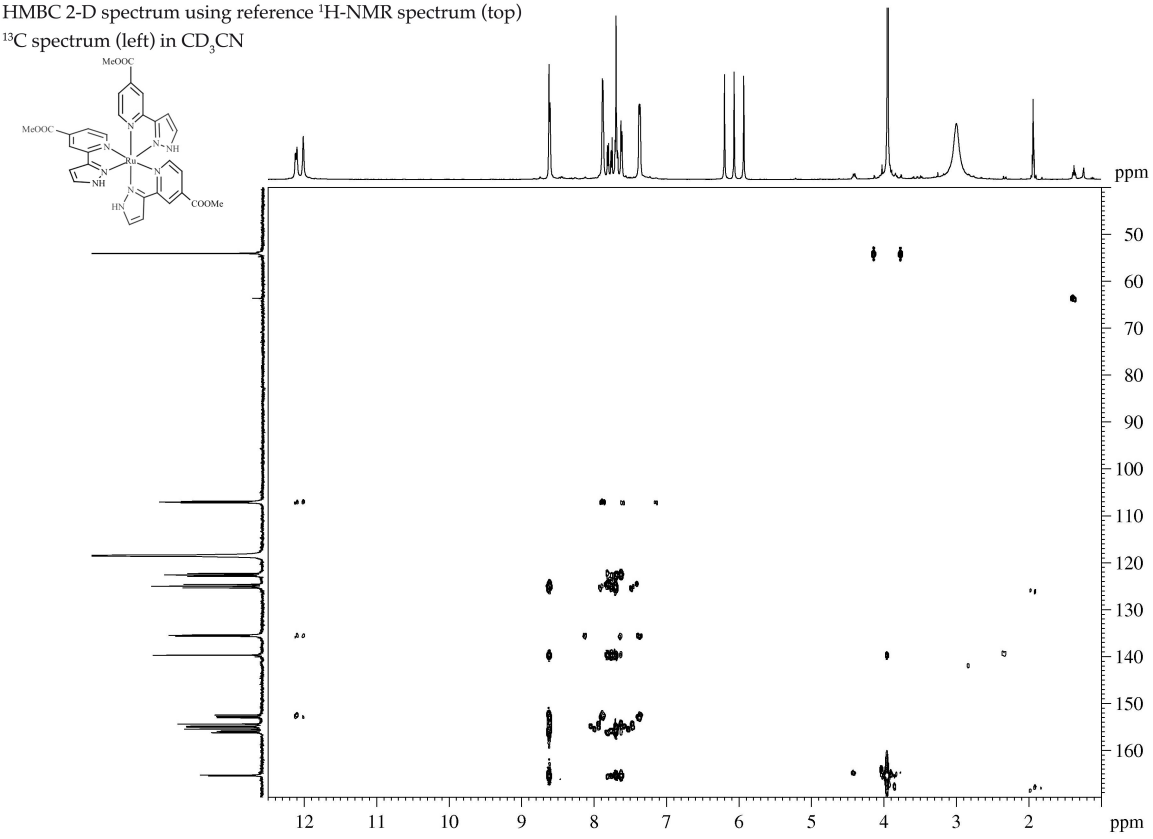

Appendix B

HMBC 2-D spectrum using reference ^{1}H-NMR spectrum (top)
^{13}C spectrum (left) in CD_3CN

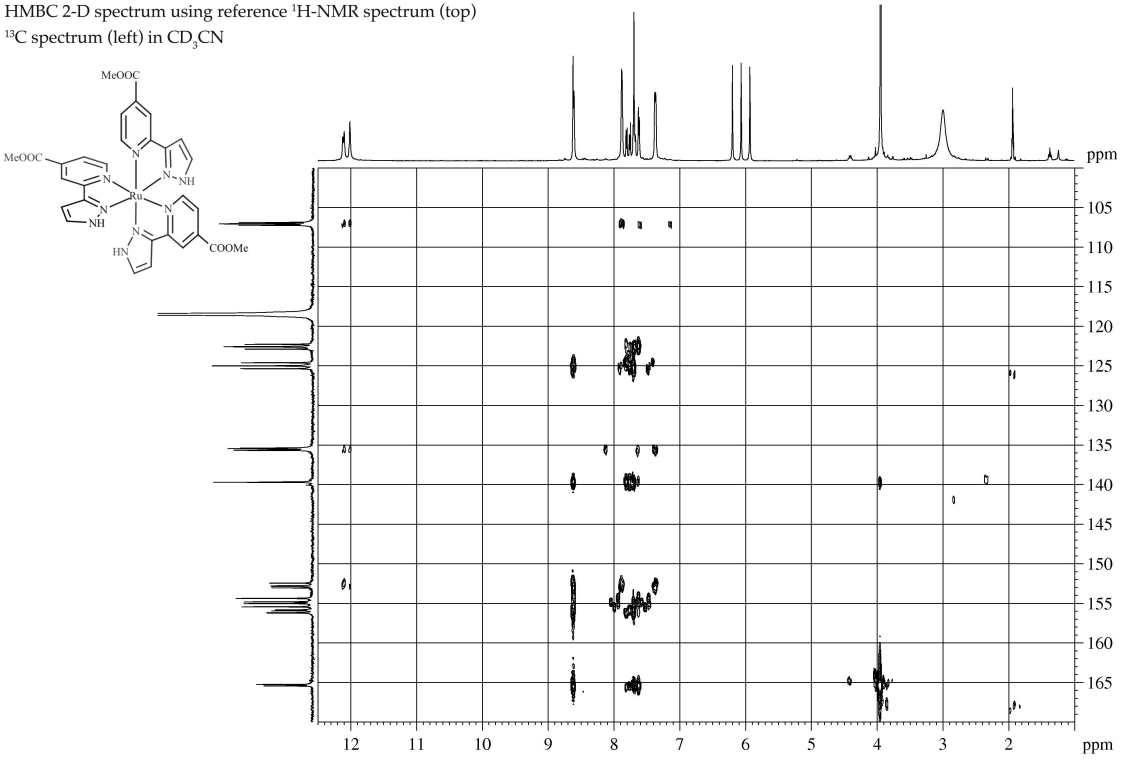

Appendix B

HMBC 2-D spectrum using reference ^{1}H-NMR spectrum (top) ^{13}C spectrum (left) in CD_3CN

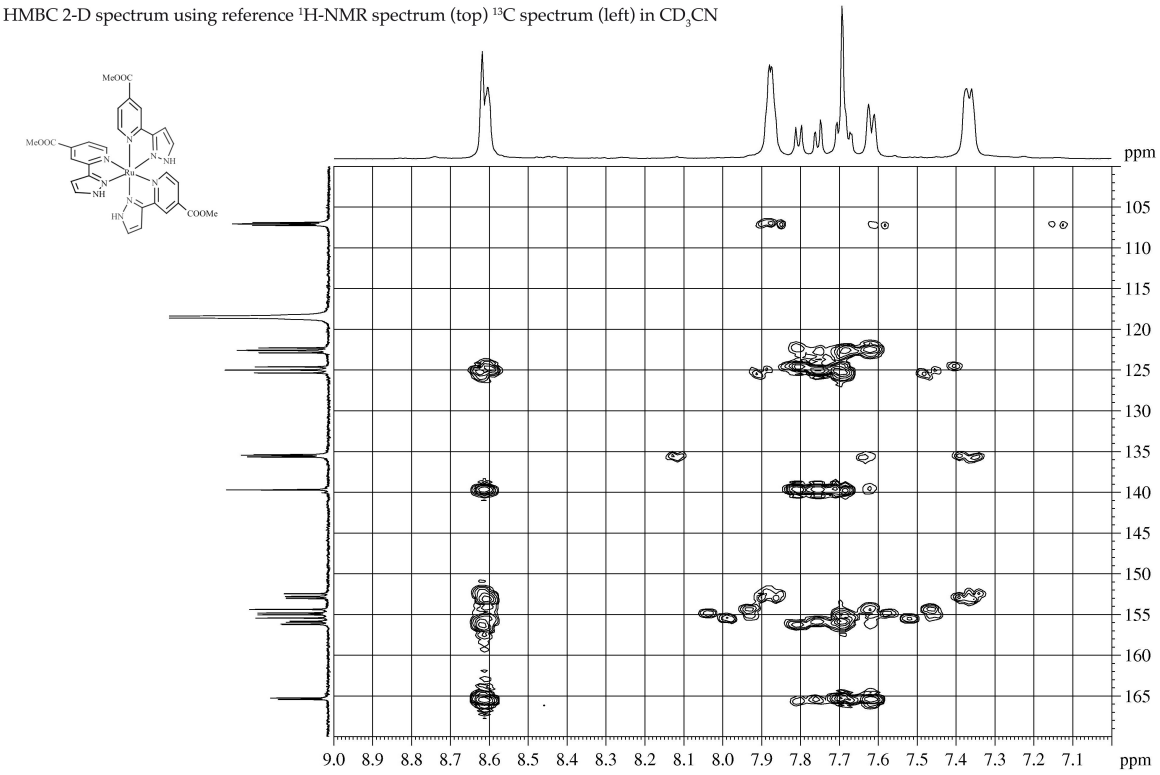

Appendix C

FTIR Spectrum of P1

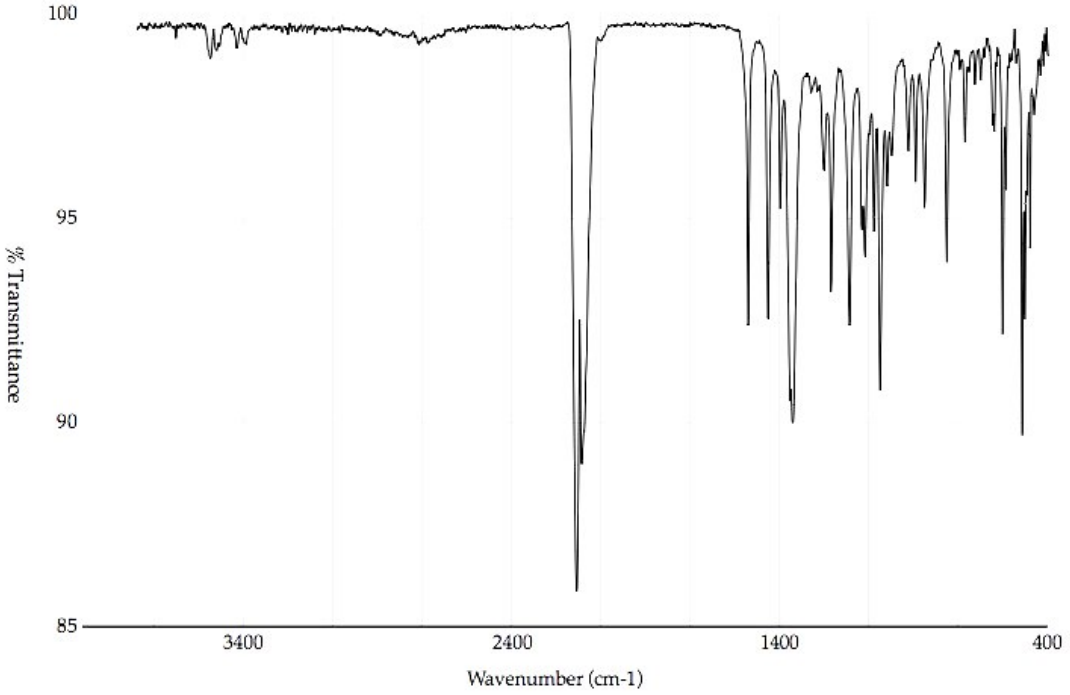

FTIR Spectrum of